Search all fields | Author name | --This Journal/Book-- | Volume | Issue | Page | Advanced search

Computer Methods and Programs in Biomedicine

Supports Open Access | About this Journal | Sample Issue Online | Submit your Article

Formerly known as Computer Programs in Biomedicine;

Get new article feed

Get new Open Access article feed

Subscribe to new volume alerts

Add to Favorites

< Previous vol/iss | Next vol/iss >

Computer Methods and Programs in Biomedicine
Volume 146, Pages 1-166 (July 2017)

Articles 1 - 18

Purchase | Export | All access types

Highlights

- Unsteady flow is considered.
- Analysis is done in non-Uniform channel.
- Copper water and Silver water nanofluids are discussed.
- Pressure gradient is evaluated.
- Exact solutions are presented.

Highlights

Volumes 41 - 50 (1993 - 1996)

Volumes 31 - 40 (1990 - 1993)

Volumes 21 - 30 (1985 - 1989)

Volume 20 (1985)

- Demonstrate a study over the selection and classification gene algorithms performance that aligned to colon cancer datasets.
- Focus on hybridization of the algorithms studied and how that reflects their accuracy and performance.
- Prove that Particle Swarm Optimization (PSO) selection algorithm, along with the functionality of the Support Vector Machine (SVM) classifier algorithm, beats other algorithms in accuracy and performance.

Support for Taverna workflows in the VPH-Share cloud platform Original Research Article
Pages 37-46
Marek Kasztelnik, Ernesto Coto, Marian Bubak, Maciej Malawski, Piotr Nowakowski, Juan Arenas, Alfredo Saglimbeni, Debora Testi, Alejandro F. Frangi
Abstract | Close research highlights | Purchase PDF - $35.95

Highlights

- We propose a method and a tool for execution of Taverna workflows on cloud resources.
- The tool integrates Taverna with VPHShare cloud platform for Virtual Physiological Human (VPH) community.
- We present use cases from VPH community and evaluate the cost and performance of executing Taverna workflows on cloud.

A PCA aided cross-covariance scheme for discriminative feature extraction from EEG signals Original Research Article
Pages 47-57
Roozbeh Zarei, Jing He, Siuly Siuly, Yanchun Zhang
Abstract | Close research highlights | Purchase PDF - $35.95

Highlights

- A low-complexity feature extraction method is proposed for EEG signal classification.
- Introducing PCA with cross-covariance method for extracting features from EEG signals.
- Efficacy of the methods are confirmed by statistical and graphical analyses.
- The method yields the utmost accuracy improving up to 0.25% than others.

A fourth order PDE based fuzzy c- means approach for segmentation of microscopic biopsy images in presence of Poisson noise for cancer detection Original Research Article
Pages 59-68
Rajesh Kumar, Subodh Srivastava, Rajeev Srivastava
Abstract | Close research highlights | Purchase PDF - $35.95

Highlights

- Presents a method for segmentation of microscopic biopsy images for cancer detection.
- The proposed method can segment the cells and nuclei of the image in presence of Poisson noise.
- The comparative analysis is presented with various standard methods in literature on various data sets.
- The proposed method is working well and of use to the Histopathologist for second opinion.

Quantifying the informativeness for biomedical literature summarization: An itemset mining method Original Research Article
Pages 77-89
Milad Moradi, Nasser Ghadiri
Abstract | Close research highlights | Purchase PDF - $35.95

Highlights

- A biomedical text summarization method is proposed.
- Itemset mining is combined with domain knowledge.

- Main subtopics are discovered to extract informative sentences.

Computer-aided prediction of axillary lymph node status in breast cancer using tumor surrounding tissue features in ultrasound images Original Research Article
Pages 143-150
Woo Kyung Moon, Yan-Wei Lee, Yao-Sian Huang, Su Hyun Lee, Min Sun Bae, Ann Yi, Chiun-Sheng Huang, Ruey-Feng Chang
Abstract | Close research highlights | Purchase PDF - $35.95

Highlights

- A computer-aided prediction system for predicting the axillary lymph node status in patients with breast cancer is proposed.
- A prediction system based on combined features of tumor surrounding tissue to predict axillary lymph node status is proposed.
- The tumor surrounding tissue would provide the useful information to predict the ALN status.

Section II: Systems and Programs

Development of an expert system for the simulation model for casting metal substructure of a metal-ceramic crown design Original Research Article
Pages 27-35
Ivan Matin, Miodrag Hadzistevic, Djordje Vukelic, Michal Potran, Tomaz Brajlih
Abstract | Close research highlights | Purchase PDF - $35.95

Highlights

- Expert system for simulation model of metal substructure for metal-ceramic crowns design is proposed.
- Blackboard architecture and data model allowed the ES to improve the design and reduce processing time and lead-time.
- Integrated RE/CAD/CAE system has been designed for IC process in dentistry.
- Design techniques and ES have been developed to generate simulation model and casting process design.

Sequence based predictor for discrimination of enhancer and their types by applying general form of Chou's trinucleotide composition Original Research Article
Pages 69-75
Muhammad Tahir, Maqsood Hayat, Muhammad Kabir
Abstract | Close research highlights | Purchase PDF - $35.95

Highlights

- Computational model is developed for prediction of Enhancer and their types.
- DNT and TNC are used as feature extraction schemes.
- Various classification algorithms are utilized.
- SVM achieved quite promising results.

Physiological closed-loop control in intelligent oxygen therapy: A review Review Article
Pages 101-108
Daniel Sanchez-Morillo, Osama Olaby, Miguel Angel Fernandez-Granero, Antonio Leon-Jimenez
Abstract | Close research highlights | Purchase PDF - $35.95

Highlights

- Studies, trials and researches published in the context of automated close-loop oxygen administration systems in adults are retrospectively reviewed.
- When compared to the conventional oxygen therapy devices, the closed-loop controllers maintain higher saturation levels, spend less time below the target saturation, and save O_2 resources.

- Closed-loop controlled oxygen therapy devices are scarce in real clinical applications.
- Main barriers such as robustness of control algorithms, fail-safe mechanisms, limited reliability of sensors, usability issues and the need for standardized evaluating methods of assessing risks are discussed.
- This study provides recommendations for future related interventions, in order to promote the wide spreading of a new generation of oxygen devices.

An intelligent support system for automatic detection of cerebral vascular accidents from brain CT images Original Research Article

Pages 109-123

Elmira Hajimani, M.G. Ruano, A.E. Ruano

Abstract | Close research highlights | Purchase PDF - $35.95

Highlights

- A RBFNN based system for automatic diagnosis of CVAs from brain CT is proposed.
- The best possible RBFNN topology, inputs and parameters are identified by MOGA.
- Symmetry features along with 1st and 2nd order statistics compose the feature space.
- 98.01% specificity and 98.22% sensitivity in a set of 1867,602 pixels are achieved.
- The proposed approach compares favourably with existing approaches.

Enhancing automatic closed-loop glucose control in type 1 diabetes with an adaptive meal bolus calculator – *in silico* evaluation under intra-day variability Original Research Article

Pages 125-131

Pau Herrero, Jorge Bondia, Oloruntoba Adewuyi, Peter Pesl, Mohamed El-Sharkawy, Monika Reddy, Chris Toumazou, Nick Oliver, Pantelis Georgiou

Abstract | Close research highlights | Purchase PDF - $35.95

Highlights

- In this paper, we present a novel technique to automatically adjust the meal-priming bolus within an artificial pancreas. For this purpose, a Run-to-Run algorithm incorporating a new control law, which avoids some of the limitations of previously proposed techniques, is introduced. Then, Case-Based Reasoning, an artificial intelligence technique which solves new problems based on the solutions of similar past problems, is employed to account for intra-subject insulin sensitivity variability.
- To evaluate the proposed technique against a non-adaptive meal-priming bolus calculator, an *in silico* evaluation using a modified version of the latest FDA-accepted UVa-Padova Type 1 Diabetes Mellitus simulator. For this purpose, 11 adult and 11 adolescent virtual subjects under real-life conditions were employed. For evaluation purposes, a novel version of the clinically validated Imperial College Bio-inspired AP controller.
- A *t*-test statistical analysis showed that, compared to a non-adaptive bolus calculator within a closed-loop controller, the proposed method has the potential to significantly improve glycemic control in diabetes management.

Continuous detection of human fall using multimodal features from Kinect sensors in scalable environment Original Research Article

Pages 151-165

Thanh-Hai Tran, Thi-Lan Le, Van-Nam Hoang, Hai Vu

Abstract | Close research highlights | Purchase PDF - $35.95 | Supplementary content

Highlights

- A *reliable* method for fall detection by combining skeleton and RGB from Kinect sensor is proposed.
- An *online* fall detection is efficiently solved thanks to the fast computation of skeleton or fall candidate detection based on grayscale motion map.
- A client-server architecture within a Kinect network is developed that is easy to scale for any space size.

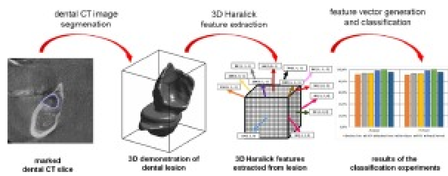

Highlights

- Using a microphone array for recording heart sound from different locations at the same time.
- Presentation of a modality for detection of active sources in the heart in a cardiac cycle.
- Sub- space based method use for localization of heart sounds.

< Previous vol/iss | Next vol/iss >

Articles 1 - 18

PubMed ▼

Format: Abstract

Full text links

ELSEVIER FULL-TEXT ARTICLE

Comput Methods Programs Biomed. 2017 Jul;146:151-165. doi: 10.1016/j.cmpb.2017.05.007. Epub 2017 May 25.

Continuous detection of human fall using multimodal features from Kinect sensors in scalable environment.

Tran TH[1], Le TL[2], Hoang VN[2], Vu H[2].

Author information

Abstract

BACKGROUND AND OBJECTIVES: Automatic detection of human fall is a key problem in video surveillance and home monitoring. Existing methods using unimodal data (RGB / depth / skeleton) may suffer from the drawbacks of inadequate lighting condition or unreliability. Besides, most of proposed methods are constrained to a small space with off-line video stream.

METHODS: In this study, we overcome these encountered issues by combining multi-modal features (skeleton and RGB) from Kinect sensor to take benefits of each data characteristic. If a skeleton is available, we propose a rules based technique on the vertical velocity and the height to floor plane of the human center. Otherwise, we compute a motion map from a continuous gray-scale image sequence, represent it by an improved kernel descriptor then input to a linear Support Vector Machine. This combination speeds up the proposed system and avoid missing detection at an unmeasurable range of the Kinect sensor. We then deploy this method with multiple Kinects to deal with large environments based on client server architecture with late fusion techniques.

RESULTS: We evaluated the method on some freely available datasets for fall detection. Compared to recent methods, our method has a lower false alarm rate while keeping the highest accuracy. We also validated on-line our system using multiple Kinects in a large lab-based environment. Our method obtained an accuracy of 91.5% at average frame-rate of 10fps.

CONCLUSIONS: The proposed method using multi-modal features obtained higher results than using unimodal features. Its on-line deployment on multiple Kinects shows the potential to be applied in to any of living space in reality.

KEYWORDS: Fall detection; Gray-scale motion map; Human monitoring; Kernel descriptor; Multiple Kinects

PMID: 28688485 DOI: 10.1016/j.cmpb.2017.05.007

LinkOut - more resources

PubMed Commons

PubMed Commons home

0 comments

How to join PubMed Commons

Computer Methods and Programs in Biomedicine 146 (2017) 151–165

Contents lists available at ScienceDirect

Computer Methods and Programs in Biomedicine

journal homepage: www.elsevier.com/locate/cmpb

Continuous detection of human fall using multimodal features from Kinect sensors in scalable environment

Thanh-Hai Tran*, Thi-Lan Le, Van-Nam Hoang, Hai Vu

International Research Institute MICA, HUST-CNRS/UMI-2954-GRENOBLE INP, Hanoi University of Science and Technology, Hanoi, Vietnam

ARTICLE INFO

Article history:
Received 12 August 2016
Revised 9 May 2017
Accepted 22 May 2017

Keywords:
Human monitoring
Fall detection
Multiple Kinects
Kernel descriptor
Gray-scale motion map

ABSTRACT

Background and Objectives: Automatic detection of human fall is a key problem in video surveillance and home monitoring. Existing methods using unimodal data (RGB / depth / skeleton) may suffer from the drawbacks of inadequate lighting condition or unreliability. Besides, most of proposed methods are constrained to a small space with off-line video stream.

Methods: In this study, we overcome these encountered issues by combining multi-modal features (skeleton and RGB) from Kinect sensor to take benefits of each data characteristic. If a skeleton is available, we propose a rules based technique on the vertical velocity and the height to floor plane of the human center. Otherwise, we compute a motion map from a continuous gray-scale image sequence, represent it by an improved kernel descriptor then input to a linear Support Vector Machine. This combination speeds up the proposed system and avoid missing detection at an unmeasurable range of the Kinect sensor. We then deploy this method with multiple Kinects to deal with large environments based on client server architecture with late fusion techniques.

Results: We evaluated the method on some freely available datasets for fall detection. Compared to recent methods, our method has a lower false alarm rate while keeping the highest accuracy. We also validated on-line our system using multiple Kinects in a large lab-based environment. Our method obtained an accuracy of 91.5% at average frame-rate of 10fps.

Conclusions: The proposed method using multi-modal features obtained higher results than using unimodal features. Its on-line deployment on multiple Kinects shows the potential to be applied in to any of living space in reality.

1. Introduction

Detecting abnormal human activities in daily life such as falling down is an important research topic in ambient assisted living [1,2]. Current commercialized solutions based on wearable sensors (e.g., accelerometer, gyroscope) are highly preferred by biomedical engineers and doctors [3–6]. However, these approaches usually generate too many false alarms due to the lack of capacities of context understanding and informative features. Other approaches rely upon ambient sensors where cameras are the most suited. Even though this research topic has been widely addressed in the literature, camera-based approaches have suffered from inheritance issues such as variations of people, illumination and viewpoint, activity phase and occlusions. Recently, with the development of low-cost depth sensors such as Microsoft Kinect, new opportunities have emerged. The depth or skeleton extracted from the Kinect sensor are valuable features to avoid the encountered issues when using conventional RGB data [7–10]. Both depth and skeleton are limited by measurable range of the Kinect sensor. They are also usually affected by noise and are unreliable due to the (self-)occlusion of the human, mostly when the human falls. These drawbacks motivate us to propose a scalable, reliable, and on-line system for human fall detection. To do this, combinations of extracted features from Kinect sensors are proposed. Moreover, technical issues that appear due to deploying the proposed techniques to a large scale environment with a Kinect sensor network, are efficiently resolved.

The data stream from a Kinect sensor provides different types of the features such as RGB, Depth, and Skeleton. Features combinations lead to efficient ways to resolve issues of the single one.

* Corresponding author at : Computer Vision Department International Research Institute MICA HUST - CNRS/UMI-2954, GRENOBLE INP Room 1005, B1 Building, Hanoi University of Science and Technology 1 Dai Co Viet, Hai Ba Trung, Hanoi, Vietnam.

E-mail addresses: thanh-hai.tran@mica.edu.vn, thithanhhai.tran@gmail.com (T.-H. Tran).

http://dx.doi.org/10.1016/j.cmpb.2017.05.007

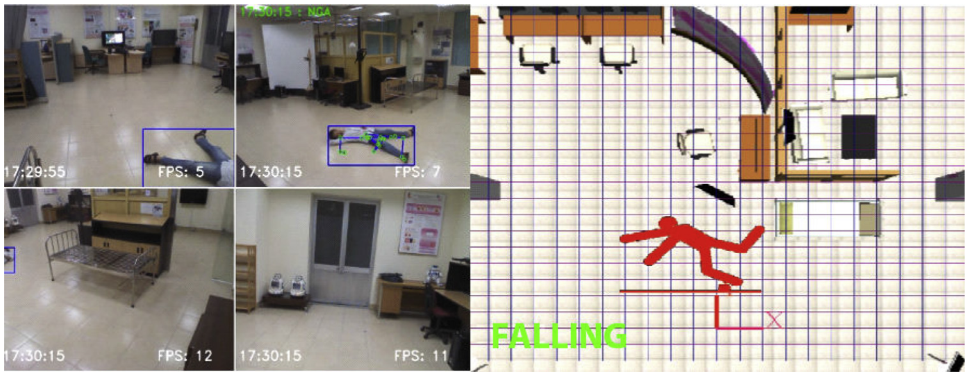

Fig. 1. Four views of Kinects overlapped by detection results (left) and a snapshot of system interface (right).

For example, we can use RGB as complement of skeleton instead of using depth. On one hand, RGB data gives important characterization of human appearance. On the other hand, RGB sensor observes a larger range than depth sensor. As a consequence, using RGB avoids missed detection at out of range of depth sensor and has better accuracy when skeleton is unreliable. However, processing on RGB features always requires a huge computational time, whereas skeleton features consist of scalar vectors, computing on these ones is very fast. In our study, the use of skeleton and RGB follows a switch strategy depending on the availability of skeleton data. A rule based detector on skeleton data is proposed so that it is called every coming frame while keeping the real-time performance. With the use of RGB data, we show that combination of gray-scale motion map and improved kernel descriptor (iKDES) outperformed state of the art works. Particularly, they are efficient descriptors for the human fall detection in order to discriminate them from other like-fall events in common daily activities.

Not only limited in detecting the human fall events using a single Kinect, we pay more attention to extend the proposed techniques to a large scale environment. The fact that in ambient assisted living application, the use of multiple cameras (or a camera network) is inevitable. The relevant technical issues related to developing a fall detection system using a Kinect sensor network are carefully resolved. Firstly, a human fall event in each Kinect is detected in a manner of continuous evolution of human postures during time. In other words, developing the applications must to deal with *on-line continuous human fall detection*. To do this, we call skeleton-based detector every frame when it is available; otherwise, we propose to detect a potential fall candidate based on the motion energy of RGB sequence. This scheme is over limitations of conventional solution which utilizes sliding windows, but the size of window is inconsistent from one fall to others. Secondly, because data stream from multiple Kinect sensors are a huge number of frames and are distributively generated, a client-server architecture is deployed. Data from each Kinect are processed separately on each client and the detection results are fused later at the server side. This architecture allows the proposed system to be scalable for any space. Fig. 1 (left panel) shows different views of Kinects overlapped by the detection results on each client. A snapshot of system interface on the server is given in Fig. 1 (right panel). Derivative technical issues such as time synchronization, view-combination from multiple Kinect sensors are deployed. The proposed techniques are intensively evaluated with different public dataset as well as state-of-the-art techniques to compare human fall detection rates. As a consequence, we demonstrate a real time and feasible human fall detection system in a large space in which actual fall events are discriminated and detected from many human like-fall events which commonly appear in daily activities.

Our main contribution therefore is four-fold, we have: (i) proposed a real-time and high accurate method for fall and non-fall classification using multimodal features from Kinect sensor (e.g. skeleton and RGB); (ii) developed a client-server system for fall detection which can be scalable for any environment; (iii) built multi-view dataset with a high diversity of fall and normal activities which could be shared for research community; (iv) empirically validated on-line this system in real environment.

The remainder of the paper is organized as follows. An analysis of the related works dedicated to fall detection is provided in Section 2. Section 3 describes the proposed method for fall detection from one Kinect while the system integration is provided in Section 4. Section 5 shows the collected dataset as well as experimental results. Some conclusions and future works are given in Section 6.

2. Related works

Fall detection attracts considerable research in the literature. There are two main trends for fall: the first trend uses wearable devices such as accelerometer, mobile phone [11] while the second one employs devices equipped in environment such as microphone and camera [12]. In this section, we focus on analyzing current works for fall detection using vision information coming from normal RGB cameras or Kinect sensors. We divide these methods into two main categories: fall detection using unimodal features and fall detection using multimodal features.

Fall detection using unimodal features: The first and the most widely used features are extracted from color images of RGB camera since RGB camera is inexpensive and easy to install. Color-based features can be computed from one sole camera or multiple cameras. Most color-based approaches based on shape features extracted from human region candidates [13,14]. First, human region is detected using a background subtraction technique (e.g. Gaussian Mixture Model). Then shape features such as width to height aspect ratio is extracted. Finally these features are used to classify a fall from non-fall using a simple thresholding technique or SVM classifier. In [15], the authors computed low level feature vectors of action sequence such as first and second derivatives, Fourier and wavelet transform and SVM technique for fall and non-fall classification. In [16], the authors proposed a method that represents human shape extracted from RGB images in Riemannian manifold. In [17], this method is improved by fusing multiple features (shape, appearance, motion) in Riemannian manifolds. Other approaches based on motion history image (MHI) and decided a fall event if the MHI has a high energy [18]. When multiple cameras with overlapped field of view are available, fall detection can be done by computing 3D human volume and analyzing this volume distribution along a vertical axis [19]. Anderson et al. utilize multiple cameras and a hierarchy of fuzzy logic to detect falls [20]. In [21], the authors proposed a multi-view fall detection system where motion is modeled by a layered Hidden Markov Model. In [22], two methods were proposed and compared using multiple cameras: the early fusion approach and the late fusion approach. In the early fusion approach, multiple views are combined to reconstruct 3D volume of the human whereas the late fusion approach is done in 2D and each camera decides on its own. The experiment showed that early fusion gives the better performance but that late fusion is more appropriate because it needs less computational power and easier to handle. RGB based fall detection depends strongly on the background subtraction result which is very sensitive to illumination changing and suffers from shadow and occlusion.

Recently, with the development of new technology, low-cost and effective RGB-D sensors such as Kinect open a new trend for fall detection. Besides color images, RGB-D sensors provide depth and skeleton information which is independent of the lighting condition. Therefore background subtraction becomes more easy and reliable. In [23], the authors proposed a method for fall detection from depth images. For this, the authors extracted a human silhouette from depth images then computed curvature scale space (CSS) features of human silhouettes at each frame and represented the action by a bag of CSS words (BoCSS). Then, they employed the extreme learning machine (ELM) classifier to identify the BoCSS representation of a fall from those of other actions. Fall detection based on depth information is robust to lighting condition. However, it is not always feasible because of the limited measurable range of depth information.

The skeleton-based works do not need to perform person detection because the skeleton is available when the person is detected. This facilitates the human action classification [24,25]. In [26], Du et al. proposed an hierarchical recurrent neural network for skeleton based action recognition that outperforms handcraft features based methods. However, this method encounters overfitting problems. To overcome the over-fitting problem, the authors in [27] proposed to mine a set of key-pose-motifs for each action class. A survey on 3D skeleton based human action classification is given in [28]. Related to skeleton-based fall detection, in [7,29], a fall is detected by applying some rules on the distance between the joints and the floor or the velocity of the joints [7] or by correlation of the skeleton joints [29]. Fall detection based on skeleton information is fast, however, it is not always feasible and reliable because of the capacity and the quality of joint tracking. In [30], the authors have performed different experiments in order to analyze the effect of joints and features for fall detection.

Fall detection using multimodal features: As each unimodal feature has its own advantages and disadvantages, some works try to combine/fuse more than one modality for fall detection. In Mastorakis et al. work [31], the authors exploited color and depth information to build 3D (height, width, depth) bounding box of the subject. Thus, two velocities in height and width are computed in order to define the fall. Recently, Kwolek et al. [32–34] combined depth information from Kinect with accelerometer mounted on the human for fall detection. In this, the accelerometer is used to indicate a potential fall while the Kinect is used to authenticate the eventual fall alert. Features extracted from depth map including a ratio of width to height of the persons bounding box, a ratio expressing the height of the persons surrounding box in the current frame to the physical height of the person, the distance of the persons centroid to the floor, standard deviation from the centroid for the abscissa and the applicate, respectively. This feature will input into a SVM to conclude if a fall happens. This method has been built and tested in an embedded system. Using additional accelerometer sensor, this method suffers from all disadvantages of wearable sensor based approaches.

Most aforementioned works focus on one room size environment, very few works consider a large environment. In [35], the authors used multiple RGB cameras in order to monitor different rooms: one camera per room.

Although, a number of approaches have been proposed for fall detection using single or multiple RGB(-D) sensors, current solutions still have some limitations. First, single camera based approach limits the monitoring space. In addition, single camera based approaches suffer from occlusion. Multiple cameras based approaches usually setup cameras with overlapped view in a small space for reconstruction of 3D human volume. It is not dedicated to extend the monitoring space. Secondly, when using RGB-D camera, current methods often based on depth or skeleton data. Skeleton is unavailable when depth is not measured. Even in the measurable range of the depth sensor, skeleton could be not well initialized and tracked, mostly when human in a non-standing posture. Then using depth and skeleton separately or combination of them are limited to the measurable range or unreliable. It still lacks the works that combine both RGB and skeleton information for fall detection. Finally, most current approaches are working with trimmed video clips (or segmented video clips). In our work, as we would like to develop an online fall detection system, the proposed solution has to deal with untrimmed videos.

3. Fall detection using multimodal features from single Kinect sensor

The Kinect sensor provides RGB, depth and skeleton data. Therefore, we will use skeleton data when it is available. If it is not the case, we will use RGB data. The flowchart of fall detection is shown in Fig. 2. According to the proposed flowchart, the fall detectors based on skeleton and RGB features are switchable depending on the availability of skeleton data. This strategy allows us to take the benefits of both the fast computations (of skeleton data) as well as a large range observation (of RGB data). Details of each detector are presented in the following sub-sections.

3.1. Skeleton-based fall detection

In [7], the authors consider all available joints of the skeleton. For each frame, they compute the average distance and the average velocity of the available joints and decide a fall event when these two values are less than pre-defined thresholds. This method gives a false alarm when a person jumping in front of the camera or when he / she is out of Kinect sensor's range. In addition, it could give multiple responses during fall.

We observe that at critical phase of a fall event, the body reduces its height (from standing height to lying height) and velocity of the body changes suddenly in the vertical direction. Therefore, we rely on these characteristics to detect a fall event. To measure the variation of distance from hip center to the ground plane and the variation of vertical speed of human body, we first extract ground plane in a current scene. Two remaining steps consist of fall feature extraction and fall detection.

In off-line phase, we extract the ground plane using the Microsoft Kinect SDK (see Fig. 3). For every frame, we re-compute this plane. If the ground plane is not found, the parameters from off-line phase will be used. We then compute the speed and distance from the hip center joint to the ground plane during a certain time. A fall is detected if the distance reduces and remains small in an interval of time and the vertical speed of the human changes a lot. The Fig. 4 shows variations of distance between hip center joint and floor plane and the vertical speed of this joint when a fall happens. We can see that from frame #113 to #145, the distance reduces from 90cm to 18cm, the vertical velocity has a peak at frame #129 corresponding to the strongest motion of the

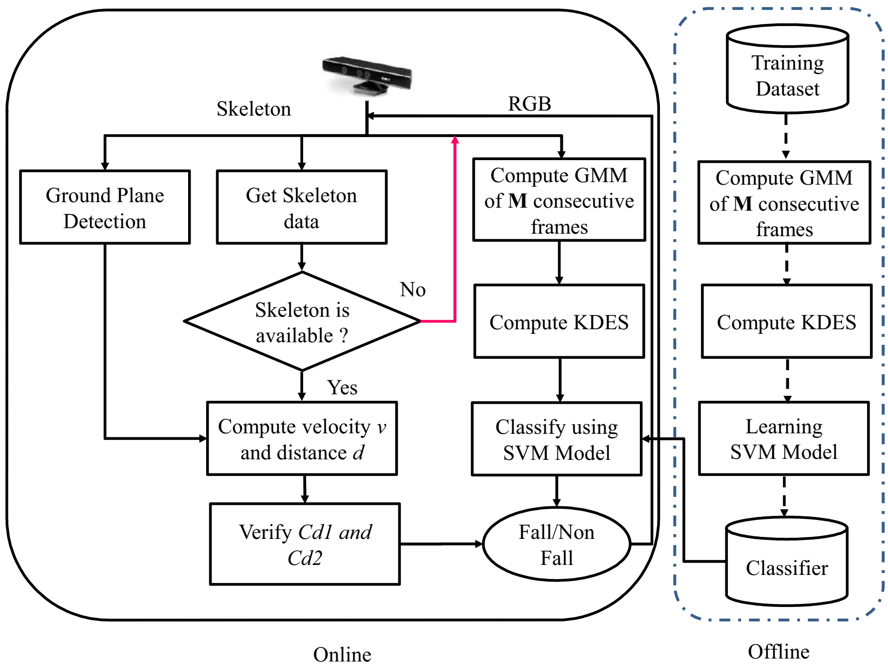

Fig. 2. Main steps of fall detection from single Kinect sensor.

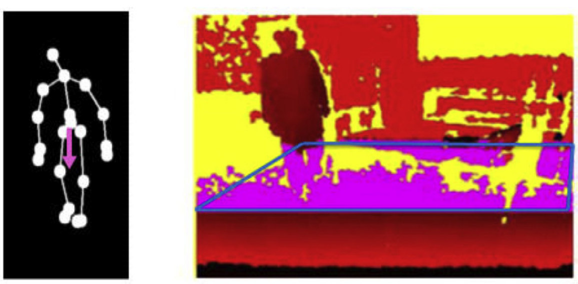

Fig. 3. Skeleton and ground plane detection. Human skeleton is on the left; we consider the height and velocity of the hip center. On the right is a depth map and the detected ground plane (in pink purple color). (For interpretation of the references to colour in this figure legend, the reader is referred to the web version of this article.)

body. This rules-based method is very fast. It does not require a long training process and it is invariant to Kinect viewpoint as well as human appearance changing.

3.1.1. Ground plane extraction

Even a number of methods have been proposed for ground plane detection, in our work, we choose ground plane detection provided by Kinect SDK because of its good performance. For each plane we have 4 values (a, b, c, d) (equation of the plane is $ax+by+cz+d=0$).

3.1.2. Fall feature computation

At time k, we compute the distance from joint center to the ground plane d_k and the speed v_k of the vertical motion of the joint center $(X_{c_k}, Y_{c_k}, Z_{c_k})$ as follows:

$$d_k = \frac{aX_{c_k} + bY_{c_k} + cZ_{c_k} + d}{\sqrt{a^2+b^2+c^2}} \quad (1)$$

$$v_k = \frac{d_k - d_{k-1}}{\delta_{k,k-1}} \quad (2)$$

where $\delta_{k,k-1}$ is the duration between two consecutive frames.

3.1.3. Skeleton based continuous fall detection

The system examines whether a fall has concluded for every frame. At kth frame, the system evaluates a range of N_d previous consecutive frames $\{k-N_d, \ldots, k\}$. A fall is confirmed if both conditions Cd_1, Cd_2 are satisfied.

$$Fall = \begin{cases} yes, & \text{if } (Cd_1 = True) \text{ and } (Cd_2 = True) \\ no, & \text{otherwise} \end{cases} \quad (3)$$

$$Cd_1 = (d_{k-m} < \theta_d \text{ with } \forall m \in [0, M_d]) \quad (4)$$

$$Cd_2 = (\exists n \in [0, N_d] \text{ so that } v_{k-n} > \theta_v) \quad (5)$$

M_d relates to the duration of motionless on the floor after fall, N_d is average fall duration. Note that the conditions Cd_1, Cd_2 are true for all cases of fall (backward, forward, literal) or from bed or during walking. This is because it verifies only the motion speed and the height of human after fall that are normally in lying position on the floor. According to this rules-based detector, the system achieves a real-time performance (15fps). We could see in the experiment section. Moreover, we set unique values to these thresholds and test for all situations of fall.

3.2. RGB-based fall detection

When the skeleton is unavailable or unreliable(because human is out of measurable range of depth sensor or human is in non-standing posture), we use RGB data. For this, we propose a kernel method. This method was described in our previous work for action classification [36]. For self contained, we present briefly this method.

We suppose that a fall candidate has happened in the interval of time from $k-N_d$ to $k-1$. The problem now is to identify the action from a sequence of frames $\{G_{k-N_d}, G_{k-N_d+1}, \ldots, G_{k-1}\}$.

3.2.1. Motion representation using grayscale motion map

We inspire the idea of Depth Motion Map firstly introduced in [37], then improved in [38] to represent an action using motion map. However, instead of using depth that could be unavailable

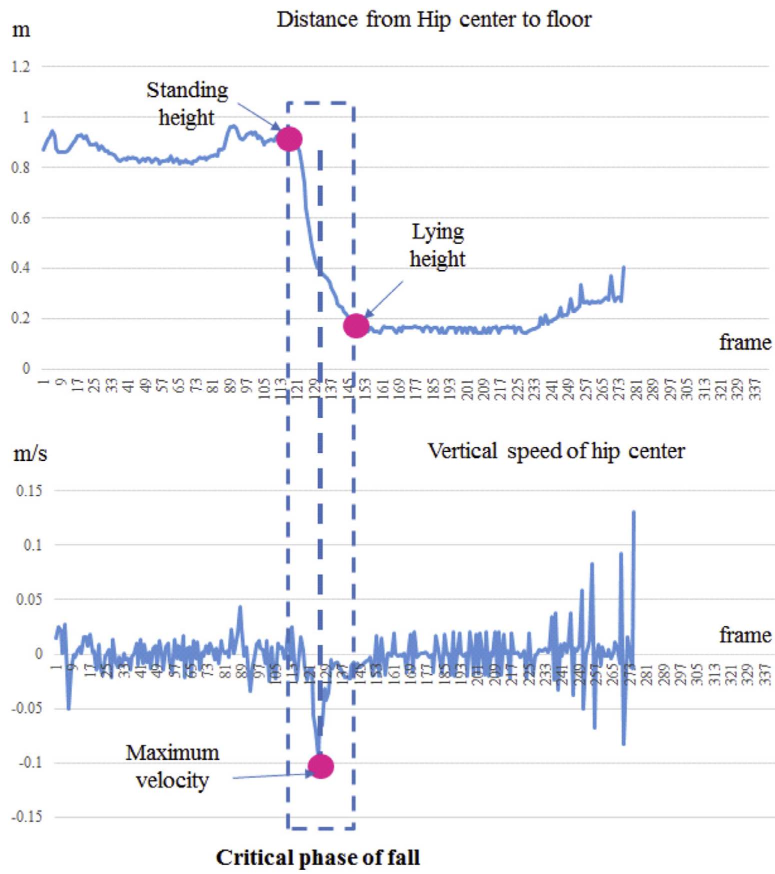

Fig. 4. Variation of the distance between hip center and floor plane and variation of the hip center speed when a fall happens.

Fig. 5. Illustration of *GMM* (right) computed from 48 consecutive frames (left) of a fall event.

when the human is out of the range of all Kinects, we compute grayscale motion map.

Given a sequence of N grayscale frames $G_1, G_2, \ldots, G_N$, the grayscale motion map is defined as follows:

$$GMM^N = \sum_{i=1}^{N-1} |G^{i+1} - G^i| \tag{6}$$

GMM stands for **G**rayscale **M**otion **M**ap. The Fig. 5 illustrates a GMM^N computed from $N = 48$ consecutive frames of a fall event.

Fig. 6 shows *GMM* computed from fall and normal activities (see description about activities in Section 5.1) from the second Kinect's view. We could see that the GMM of each activity differs from each other due to the position where the activity takes place and the movement of the person. The consistency of GMM of each activity class is illustrated in Fig. 7.

3.2.2. Computation of kernel descriptor from GMM

Once the *GMM* was computed, we extract improved gradient kernel descriptor (GiKDES) from this map to input into a SVM classifier for action identification. This method has been given the acronym GMM-GiKDES-SVM. Kernel descriptor has been introduced for the first time in [39]. We have made two improvements on this descriptor to make it more invariant to rotation and scale change [40]. Our improvements outperform the origi-

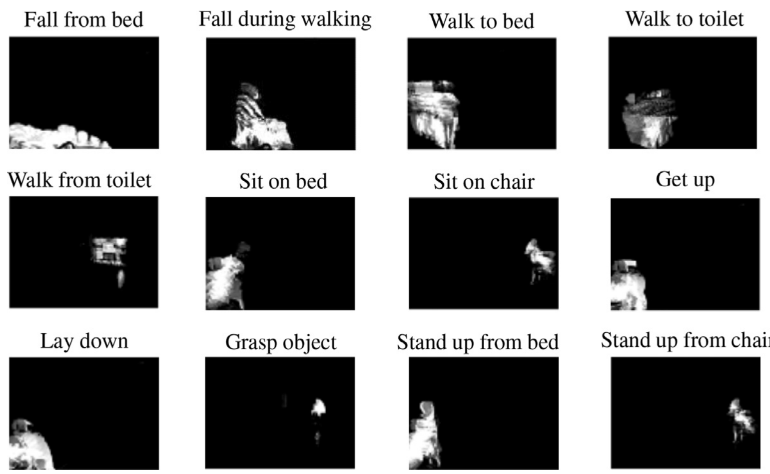

Fig. 6. *GMM* computed from different types of activities.

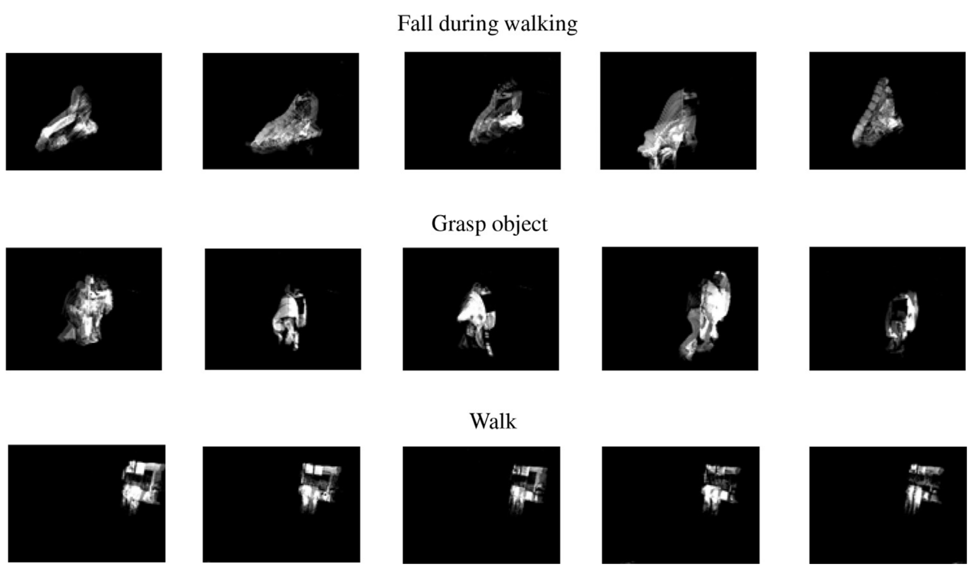

Fig. 7. GMM computed from different samples of the same activity.

nal kernel descriptor in many datasets of hand posture [41], person re-identification [42] and action recognition [36]. To consolidate the paper, we summarize briefly the computation of improved kernel descriptor. The reader could refer to the original paper [40] for more detail. The computation of kernel descriptors consists of three levels.

- At pixel-level, we compute gradient vector for every pixel in the image and *normalize its orientation (the first improvement)*. This makes our descriptor invariant to rotation at patch level compared to the original descriptor introduced in [39].
- At patch-level, we generate patches from the image with *adaptive patch size (the second improvement)*. For each patch, patch feature is computed based on the definition of match kernel. Compared to [39] which generates with fixed patch size, our descriptor will be invariant to scale change.
- At image-level, a pyramid structure is used to combine patch features. Given an image, we apply the efficient match kernel technique to create final representation from lower levels features.

All normal activity sequences are grouped into non-fall fold. The kernel descriptors are computed for all video sequences from fall and non-fall folds and input into a linear SVM classifier for training and testing.

3.2.3. RGB based continuous fall candidate detection

For a real application, data stream from the Kinect sensor comes consecutively. Because the skeleton-based detector can run real-time, we do not need further process. However, for the RGB-based detector, to avoid calling every frame for the GMM-GiKDES-SVM module that is quite time-consuming, we determine whether a fall candidate happens from continuous frames. Based on the assumption that the environment is fixed and the human stays motionless in a duration after falling, the motion map computed from the consecutive frames in this duration has very small value or even zero. We detect motionless moment as follows:

- At every coming frame, we compute the motion map GMM^N on RGB image from N consecutive frames just before the current frame using Eq. (6). The value N is chosen by experiment.
- Then we compute the total energy of the motion map.

$$E_{GMM^N} = \sum_{x=0,W-1,y=0,H-1} GMM^N(x,y) \tag{7}$$

where W, H are the width and height of image respectively.

- Finally, we verify and decide according to the following condition:

$$FallCandidate = \begin{cases} no, & \text{if } E_{GMM^N} \geq \theta_{GMM^N} \\ yes, & \text{otherwise} \end{cases} \tag{8}$$

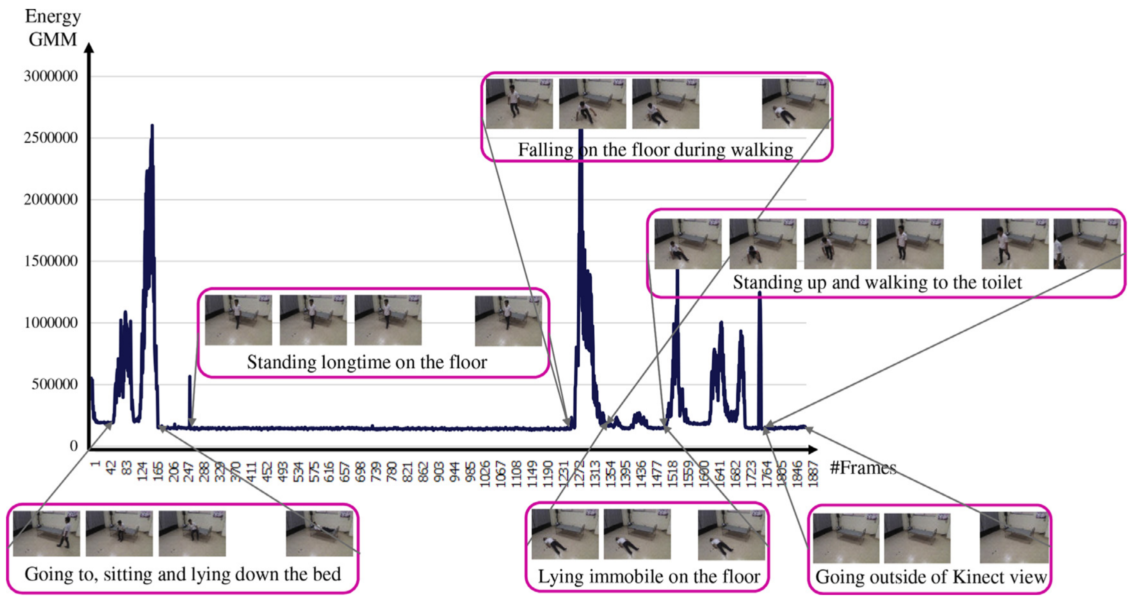

Fig. 8. Analysis of GMM energy of a video sequence containing continuous actions: walking to the bed, sitting down the bed, lying down the bed, standing up, falling on the floor, staying immobile on the floor, standing up and walking our of Kinect view.

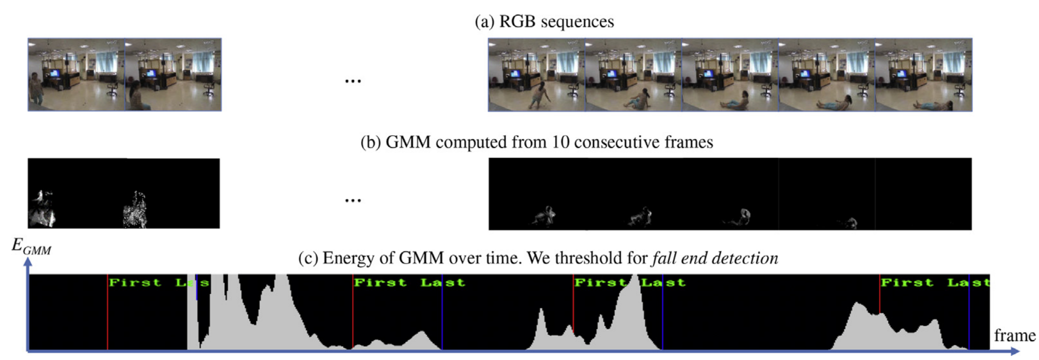

Fig. 9. Verification of *GMM* energy for fall candidate detection. (For interpretation of the references to colour in this figure legend, the reader is referred to the web version of this article.)

Fig. 8 shows variation of E_{GMM^N} during time. When there is no motion (because of the human staying immobile or no human in the room), the value of E_{GMM^N} is small. Basing this analysis, we choose the value of $\theta_{GMM^N} = 20,000$ in our experiment.

The Fig. 9 shows a RGB sequence (the first row), the corresponding GMM^N computed from every 10 consecutive frames (the second row) and the energy of GMM^N overtime (the third row). Following our proposition, we select the moment at which E_{GMM^N} smaller than a threshold θ_{GMM^N} and consider that moment as the end of an potential fall candidate. In the third row of Fig. 9, blue lines represent potential fall candidates. We will backward N_d frames before, compute GMM, GiKDES and recognize the type of activities using SVM classifier. The red lines in Fig. 9c represent the beginning of fall candidates.

4. Fall detection using multiple Kinect sensors in a large environment

4.1. Client-server architecture

We have presented the method for fall detection from single Kinect sensor. In a large scale, we have to setup multiple Kinect sensors and integrate all into an unified framework. Our system has client-server architecture (see Fig. 10). Each client processes independently data from one Kinect sensor.

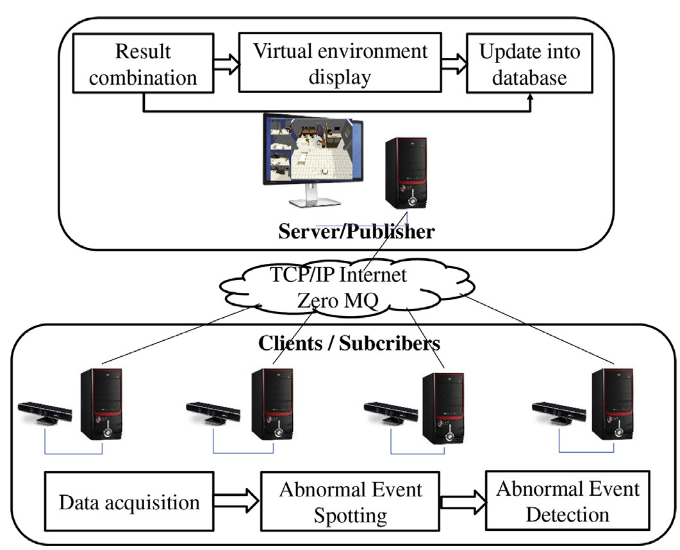

Fig. 10. Distributed architecture of the proposed system.

The main processing includes data acquisition and activity classification. Output of these modules will be sent to the server computer which receives and performs fusion of results. We display final results on the monitor and update into database for further processing. For the connectivity purpose, all of the computers are connected to a LAN network with an Ethernet cable.

To run the system, firstly, we do the time setting for all clients and server PC to ensure as much as possible temporal synchronization. Then we start manually fall detection module at each client computer. If a fall is detected from a client computer, a message will be sent to the server computer using TCP/IP protocol with ZMQ library. The structure of a message frame is {ID, P_x, P_y, EventID} where $ID \in \{1, 2, 3, \ldots, K\}$ is the client index, (P_x, P_y) is the position in image where the event happened, EventID $\in \{F, NF\}$ is the event label (F, NF stand for Fall and NonFall respectively).

In our configuration, the transmission time of a single message is about 40 ms. At server side, a collection module gets all information sent from clients and makes a fusion every 100 ms.

4.2. Late fusion technique

Among many type of fusion techniques, we choose late fusion because late fusion system could scale up easily without requiring re-training if further Kinects are to be integrated and it provide higher degree of modularity.

Algorithm 1 : Fusion of fall detection results at server side.

$t_f = 0$; $Falled = 0$; $t_{previous} = 0$;
$T_{scan} = 0.1(s)$; $T_{timeout} = 5(s)$;
while true **do**
  $t = getcurrentime()$;
  $\delta_{tr} = t - t_{previous}$;
  $t_{previous} = t$;
  if $(\delta_t = T_{scan})$ **then**
    $\delta_{tf} = t - t_f$;
    for mgs_i **do**
      $t = getcurrenttime()$;
      if $(Falled! = 1)$ && $(\delta_{tf} < T_{timeout})$ **then**
        FallAlarm(); $t_f = t$; $Falled = 1$;
      end if
      if $(Falled! = 0)$ && $(\delta_{tf} > T_{timeout})$ **then**
        FallAlarm(); $t_f = t$;
      end if
    end for
  end if
end while

The technique to fuse detection results from multiple Kinects is described in Algorithm 1 and illustrated as in Fig. 11. The main principle of the algorithm is that a fall event is concluded if at least one EventID of coming messages in this period of time has value "Fall". Then the system displays the event label and corresponding human avatar on the screen (an illustration in Fig. 11). To avoid multiple responses, we generate only one fall warning in a duration of $T_{timeout}$ even there are several messages of fall coming from different clients or one client in this period. In our experiment, because one fall happens normally during at least 5s, and there is only one person in the room so there are no more than two falls during this time. So we set $T_{timeout} = 5$s.

Table 1
Quantitative specification on Dataset - A.

Class	Activity	Video segments	Total
1	Human fall	30	30
2	Crowching down	8	
	Bending over	7	40
	Getting seated	9	
	Lying down	16	

Table 2
Quantitative specification on Dataset - B.

Class	Activity	Video segments	Total
1	Human fall	99	99
2	Walking	53	
	Sitting down	58	143
	Standing up	28	
	Housekeeping	4	

5. Experiments and discussions

5.1. Video datasets for fall detection

5.1.1. Dataset - A

The first dataset URFD[1] was used in [33] which contains 70 sequences (30 falls + 40 daily living activities). Daily living activities include sitting down, crouching down, picking up an object from the floor and lying on the sofa. Two types of fall were performed by five persons, namely from standing position and from sitting from chair and observed by two overlapped view's Kinects. RGB, depth information and accelerometer are provided. This dataset does not provide skeleton data. Quantitative specification on this dataset in given in Table 1. In [33], the authors used depth or combined depth and accelerometer data for fall detection. Methods in [16,17] use RGB data while [3] used only accelerometer data. In our work, we use RGB data. We will compare our method of fall detection based on RGB data to all of these methods.

5.1.2. Dataset - B

The second dataset LE2I[2] was used to test the method presented in [15]. This is a single view dataset which contains 191 RGB video sequences. This dataset presents main difficulties we can find at an elderly home environment such as variable illumination, occlusions, cluttered and textured background. The subjects performed various normal daily activities and falls at different location such as Home, Coffee Room, Office, Lecture Room. In this work, we evaluate our algorithm based on RGB data and compare with [15] following the P1 protocol (the training and the test subsets were built with videos from the locations Home and Coffee room). This dataset is used to validate the robustness of methods to location changes. Quantitative specification on this dataset in given in Table 2.

5.1.3. Dataset - C

The third dataset MICAFALL-1[3] is prepared by ourself. We have built a simulated studio of size (9.2mx8.8m) with office background. It is simulated to have a living room and a toilet. The living room is equipped with a bed, a cupboard, a chair and surrounding office objects. The room could be illuminated by neon lamps on the ceiling or by sunlight. This lab-based environment tries to simulate as much as possible a living space of a flat.

1 http://fenix.univ.rzeszow.pl/~mkepski/ds/uf.html.
2 http://le2i.cnrs.fr/Fall-detection-Dataset.
3 http://mica.edu.vn/perso/Tran-Thi-Thanh-Hai/MFD.html.

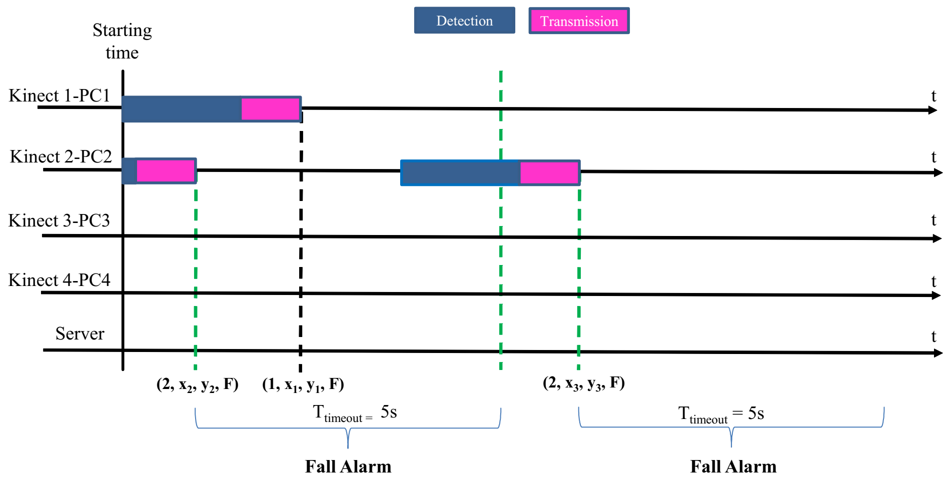

Fig. 11. Fusion result at server side. (For interpretation of the references to colour in this figure legend, the reader is referred to the web version of this article.)

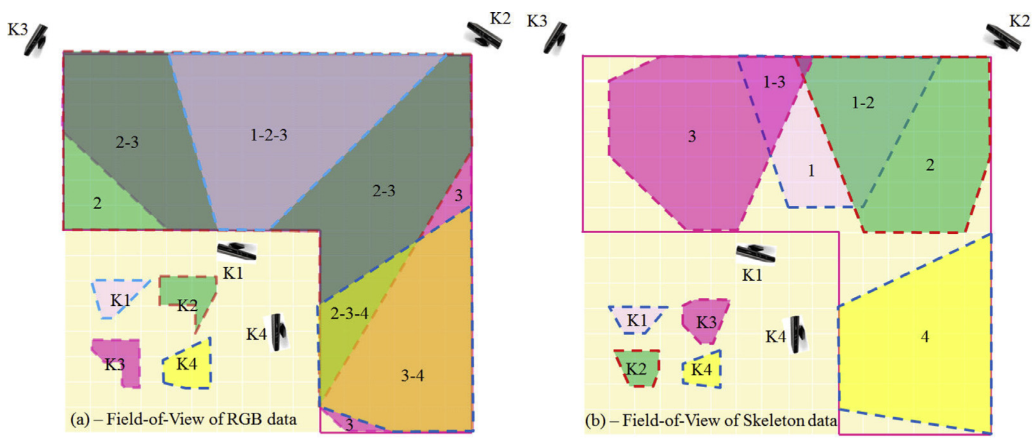

Fig. 12. Overlapped views of four Kinect sensors: RGB at the right and Skeleton at the left. Each color shows the region observed one or more Kinects.

Based on room layout, we installed four Kinect sensors at places to observe entire space (see Fig. 1). The objective is to observe space with the minimal number of sensors. Each Kinect is plugged to a nearby PC. We note that depth and skeleton information are not always available at all positions inside the room. Fig. 12 shows the field of view of each Kinect sensor.

We invite 20 subjects aging from 25 to 35 years old to make 40 falls (20 falls during walking and 20 falls from bed) and 200 daily activities (walking from door to bed, walking from bed to toilet, walking from toilet to bed, gasping object, sitting on the chair, sitting on the bed, get up from the bed). The order of performing these activities could be different from one subject to others and from one trial to another one. In the Dataset-C, subjects performed activities following a scenario so theirs skeletons are well initialized and tracked. Most falls during walking happened in the view of Kinect 2 or Kinect 3. A half of the dataset is used for training, the remaining half is for testing.

5.1.4. Dataset-D

The main goal of building the Dataset-D is to evaluate the roles of combining RGB and Skeleton and the role of using multiple Kinects for fall detection in a large scale space. To this end, we ask subjects to perform activities (including falls and normal ones) at some specific positions. To show the role of RGB at unmeasurable range of the Kinect, falls are performed at positions where the skeleton is not observable (Fig. 12b). To show the advantages of combining multiple Kinects, we ask participants to perform falls at frontier positions observable by more than one Kinect (Fig. 12a). These positions are very sensitive because one Kinect could observe only one part of the human body and the whole action of the human is not observed.

We invited 4 subjects aging from 30 to 40 years old to make 95 free falls and 206 daily activities (walking, bending, grasping, jumping, sitting on the chair, sitting on the bed, standing up) at different positions in these regions. Among the 95 falls during walking, there are 32 falls at unmeasurable range of all Kinects , so skeletons are not available; 63 falls at frontier regions observed by more than two Kinects. The order of performing these activities could be different from one subject to others and from one trial to another one.

For both Dataset-C and Dataset-D, all Kinects are set to 20fps with resolution of 640x480. They capture the scene at the same time. All data (depth, RGB, skeleton) are then processed to be synchronous using Network Time Protocol (see Fig. 13). Quantitative specification on this dataset is given in Table 3. Both Dataset-C and Dataset-D are made available to the scientific community through a website [43] (Tables 3 and 4).

5.2. Parameters setup

The proposed framework is warped by a C++ program. As PC clients have different hardwares, the processing time will be different on each PC. In addition, the processing time will depend also on which module of fall detection (skeleton based or RGB based) will be called. Therefore, to ensure the equivalence among Kinects, we use interval of time instead of number of frames. In

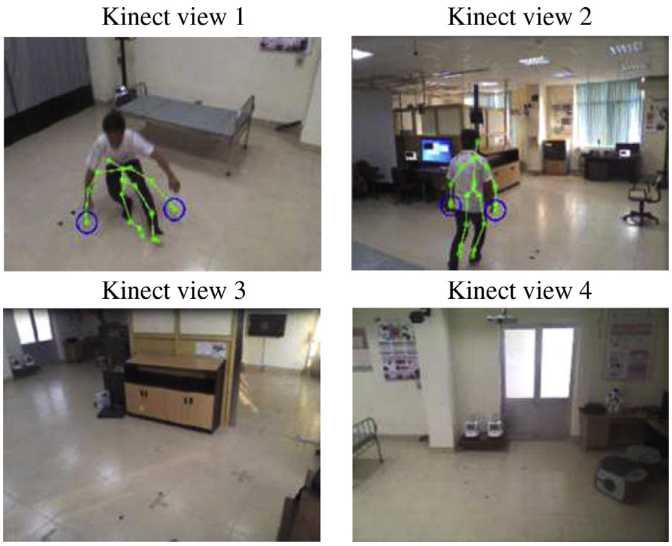

Fig. 13. Synchronization of four Kinect views: Skeleton is displayed overlapped on the corresponding RGB image. In falling postures, skeleton is not really reliable.

Table 3
Quantitative specification on Dataset -C.

Class	Activity	Video segments	Total
1	Falling from bed	20	40
	Falling during walking	20	
2	Walking	60	
	Sitting	60	
	Lying on bed	20	200
	Bending	20	
	Standing up	40	

Table 4
Quantitative specification on Dataset -D.

Class	Activity	Video segments	Total
1	Falling during walking at overlapped regions	63	
	observed by at least two Kinects		95
	Falling during walking at unmeasurable range	32	
	of any Kinect		
2	Walking	95	
	Bending	8	206
	Standing up	95	
	Jumping	8	

Table 5
Performance of fall detection using Skeleton (%) on Dataset-C.

Kinect view	Acc	Pre	Sens	Spec
Kinect 2	95.00	85.00	94.44	95.16
Kinect 3	96.70	88.88	80.00	98.76

our experiments, we set $N = 10$, $\delta_{M_d} = 5$s corresponding to time duration of motionless after almost fall, $\theta_d = 25$ cm corresponding to the height of human body w.r.t floor plane at lying position , $\theta_v = 0.01$, $\delta_{N_d} = 3$ s (time duration of a fall following [2]). These parameters are chosen by experimental observations. The value of θ_{GMM^N} is chosen based on analysis of GMM energy variation of a static scene in an interval of time. Ideally, this value could be zero. However, as illumination changes often in reality, we empirically choose $\theta_{GMM^N} = 200000$ which is the suitable value at *no moving* scene (see Fig. 8). From δ_{M_d} and δ_{N_d}, we can compute the corresponding number of frames M_d, N_d. Measurements of evaluation are Accuracy, Precision, Sensitivity, Specificity as used in [3,33].

Table 6
Performance comparison (%) of fall detection using Skeleton.

Method	Acc	Pre	Sens	Spec
Method in [7]	41.86	26.32	31.25	48.15
Our skeleton based method	**93.02**	**100.0**	**81.25**	**100.0**

5.3. Single view evaluation

5.3.1. Evaluation of skeleton-based fall detection

This evaluation is done with Dataset-C. The second Kinect observes twenty falls. Three falls were mis-detected. The reasons come from unavailability (one fall happened at the position far from measurable range of the Kinect), or unreliability of the skeleton data (skeletons from one fall from bed and one fall in front of the toilet are difficult to be initialized). The third Kinect observes ten falls, two falls were missed by the same reasons. Table 6 shows the overall results of skeleton based method. It takes only 20ms to detect one fall event when running on a PC with Core I7, CPU 3.4 GH. No false alarms have been detected with the first and the fourth Kinects.

We compare the performance of our fall detection based on skeleton with the method proposed in [7]. In [7], the authors use distance or average velocity of joints of human skeleton for fall detection. We use the software downloaded from [44]. As this software requires to connect directly with the Kinect sensor, we then run two programs (our method, the method in [7]) at the same time. The Kinect 2 observes the same scene. Four people have been invited to play fall and normal activities. Totally, we have 16 falls and 27 normal activities (including 7 walkings, 7 bendings to grasp object, 10 sittings on the floor, 3 sittings on the chair). All activities have been played in the measurable range of the Kinects so that skeleton information is achievable.

We found that our method does not give any false alarm (Spec = 100.0%). Among 16 ground-true falls, our method mis-detected 3 falls due to the self-occlusion of human during fall and short time of motionless. The method [7] gave lot of false alarms, mostly in case of sitting quickly on the floor then stand up. It mis-detected lots also due to some pres-fixed thresholds that not really suitable in our context.

5.3.2. Evaluation of RGB based fall detection

Evaluation on Dataset - A. We conducted the same test (10-fold cross validation) as in [33]. The dataset - A contains different types of falls: forward, backward and lateral. However, our technique based on motion map and kernel descriptor is independent of the fall style. We compare our method with other methods [3,16,17,33]. In [3], accelerometer sensor is worn on human body and a thresholding method on accelerometer data is used for classifying a fall from non-fall. In [33], the authors detect first fall candidate based on accelerometer data then extract shape features from depth to input into a SVM for fall and non-fall classification. In [16,17], the authors represented shape, motion and appearance features of the human action on Riemannian manifolds. All of these features are extracted from RGB channel.

Table 7 shows our method outperforms [3,17,33] in term of Accuracy, Precision and Specificity. This shows our method works very well on solely RGB data. All falls have been correctly detected (Sens = 100%). Our method avoids better false alarms (Spec = 99.23%) in comparison with [33] (Spec = 80%). Evenly, our method is better than [33] when they combined depth and accelerometer data. This could be explained by the fact that depth data could

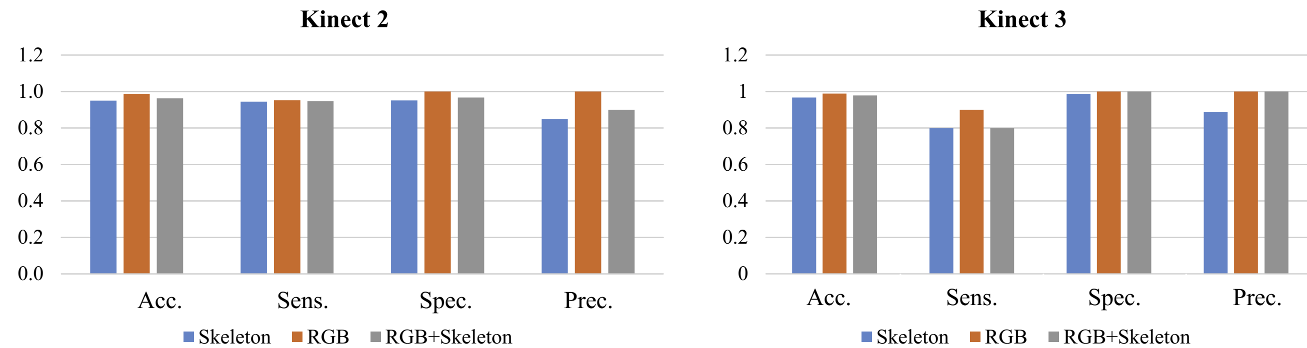

Fig. 14. Performance comparison using RGB, Skeleton, RGB+Skeleton on Dataset-C.

Table 7
Performance of fall detection (%) on Dataset - A.

Method	Data type	Acc	Pre	Sens	Spec
Bourke et al. [3]	Accl.	95.00	90.91	100.0	90.00
Kwolek et al. [33]	Depth	90.00	83.30	100.0	80.00
Kwolek et al. [33]	Depth + Accl.	98.33	96.77	100.0	96.67
Yun et al. [16]	RGB	–	–	96.77	89.74
Yun et al. [17]	RGB	–	–	100.0	97.25
Our proposed method	RGB	**99.37**	**96.77**	100.0	**99.23**

Table 8
Performance of fall detection (%) on Dataset - B.

Method	Acc	Pre	Sens	Spec
Charfi et al. [15]	**99.61**	94.23	**98.00**	**99.69**
Our proposed method	97.90	**96.00**	97.95	97.87

Table 9
Performance of fall and non-fall classification (%) using GMM-GiKDES-SVM on Dataset -C.

Kinect view	Acc	Pre	Sens	Spec
Kinect 2	98.75	100.0	95.24	100.0
Kinect 3	98.90	100.00	90.0	100.0

Table 10
Comparison of computational time.

Method	Average computational time (ms) per fall activity
Skeleton	20
RGB	1600
RGB+Skeleton	108

be missing with strong sunlight. In addition, from our experiences, depth data at human hair and foot regions are usually missing. Kwolek and Kepski [33] computed features based on human bounding box which could be affected by this missing data. Our method based only on the motion map computed from a sequence of images, and the kernel descriptor is robust then it avoids better false alarm. The method based only on accelerometers [3] gives much more false alarms (Spec = 90%) than our method (Spec = 99.23%). This is quite evident because a fall decision based only on accelerometer could be easily confused with a fall when the human moves a lot.

Evaluation on Dataset - B. We compare our method GMM-iGKDES-SVM for fall detection based on RGB data with [15] on Dataset - B. In [15], the authors computed low level feature vectors of action sequence such as first and second derivatives, Fourier and wavelet transform and SVM technique for fall and non-fall classification. We apply the evaluation protocol P1 (using a part of fall and non-fall from Home and Coffee room subset for training and the remaining for testing). Environment of these two locations are very different. The human could be fallen down in any direction. The objective of testing methods on this dataset is to validate their robustness to location changes. The method in [15] computed shape features from extracted bounding box of the human. This depends strongly on background subtraction result. Tab. 8 shows the comparison result. We see that our method obtains comparable performance and independent of the background subtraction.

Evaluation on Dataset-C. Table 9 shows the result obtained by our RGB based method on the Dataset-C. We found that a combination of GMM-GiKDES-SVM is good enough for fall detection under different viewpoints of Kinect sensor. No false alarms were generated (Spec = 100%) for both views. All falling from bed activities are correctly detected. One time a falling during walking was detected as falling from bed. This is because the position at which the fall happens is near from bed and the critical phase of fall was quite long. Our algorithm takes only a fix interval of time (fall duration) so we could not take the images at the beginning of critical phase where the person was in standing position. Therefore, the GMM of this falling during walking in this case is quite similar to GMM of falling from bed height. The fall-like activity (bending and grasping) is also correctly classified and unconfused with falls.

5.3.3. Evaluation of combining RGB and skeleton based fall detection

As analyzed previously, fall detection using skeleton data is fast (20 ms), but limited in the measurable range of Kinect sensor or unreliable. We have conducted our evaluation on Dataset-D. In this dataset, 32 falls were done at unmeasurable ranges of any Kinect. 27 falls have been correctly detected by at least one Kinect using GMM-iKDES-SVM, no false alarm was detected. This means that without using RGB information, the system will miss all falls at these locations.

Beside, even in regions where skeleton is available, when human falls, its skeletons is unreliable and unstable. In that case, rules (3) for fall detection are not satisfied. RGB based fall detection will help to avoid this mis-detection.

However, fall detection based on GMM-iKDES-SVM is quite consuming (1.6s on a PC with Core I7, CPU 3.4GHz). Therefore, the use of this detector at locations having skeletons is unnecessary. Our fusion technique presented in the flowchart of Fig. 2 helps to speed up the detection module fifty times faster (see Table 10). Fig. 14 shows results obtained using single channel or both on the Dataset-C. For the second Kinect's view, the combination gives better performance than using sole skeleton, although this reduces the performance compared to the method using RGB. The performance decreases due to the unreliability of human skeleton during fall. For the third Kinect's view, the performance after combination re-

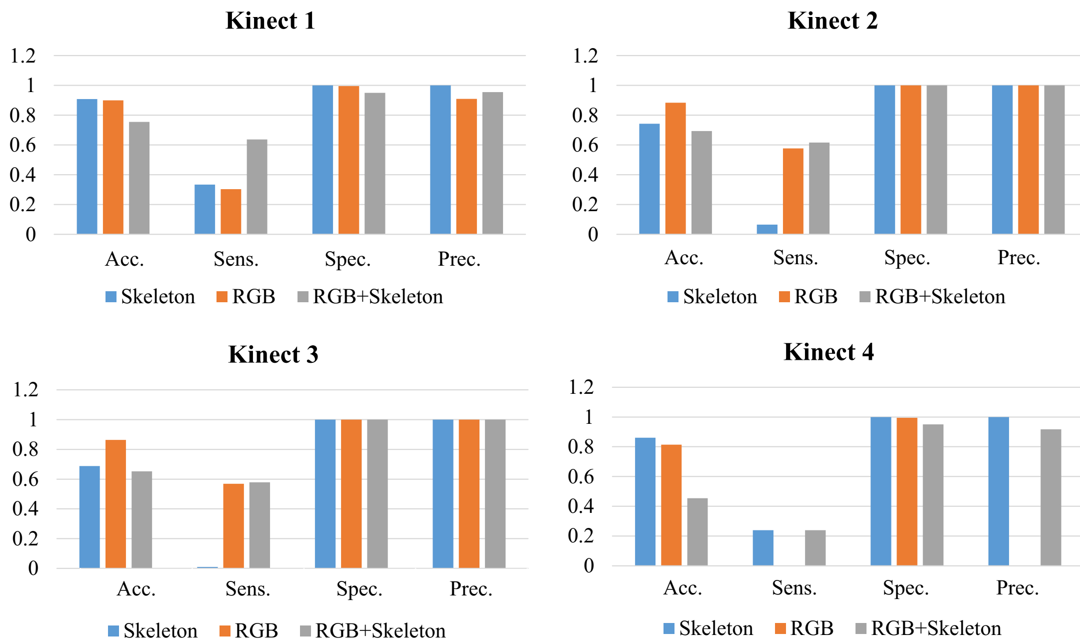

Fig. 15. Performance comparison using RGB, Skeleton, RGB+Skeleton on Dataset-D.

Table 11
Evaluation of fusing multiple Kinects on Dataset-D.

Eval (%)	K1	K2	K3	K4	K24	K34	K123	All Kinects
Acc.	94.56	89.43	86.71	85.71	91.55	88.03	94.68	**96.01**
Sens.	63.64	61.54	57.89	23.91	70.51	63.16	84.21	**88.42**
Spec.	99.51	100	100	99.51	99.51	99.51	99.51	**99.51**
Prec.	95.45	100	100	91.67	98.21	98.36	98.76	**98.82**

mains the same. Therefore, to speed up the system, in on-line running, we will apply RGB and skeleton based fall detection.

Fig. 15 shows obtained performance for each Kinect in the Dataset-D. As we explained previously, in this dataset, the skeleton was not well initialized and tracked. As consequence, without using RGB information, skeleton based fall detection has very low sensitivity (e.g. 6.4% by Kinect 2, 1% by Kinect 3). Combining Skeleton with RGB increases substantially to 57.89% and 61.53% respectively.

5.4. *Evaluation of advantages of using multiple Kinects in a large space*

In this section, we would like to evaluate advantages of using multiple Kinect sensors in a large space. Using one Kinect, we could recognize well a fall happening at the center view of the Kinect. However, when a fall happens at the boundary view, one Kinect can not observe the whole activity (or the whole human body). Then recognition based on single view has a low rate (e.g. from 23.91% to 63.63% when using both RGB and skeleton).

In Dataset-D, as mentioned previously, we have asked subjects to perform falls at boundary locations of two and/or more Kinects (K2+K4, K3+K4, K1+K2+K3) (Fig. 12). We then make late fusion of several Kinects. Table 11 shows that fusing results from multiple Kinects give better sensitivity. For example sensitivity is of 61.54% using single Kinect 2, 23.91% using Kinect 4 but 70.51% using both Kinect 2 and Kinect 4. Sensitivity is of 63.64% using single Kinect 1, 61.54% using Kinect 2, 57.89% using Kinect 3 but 84.21% using three Kinect1 Kinect 2 and Kinect 3. Using all Kinects, we obtained the highest sensitivity (88.42%). It is noted that this sensitivity is computed only for falls happening at *difficult* locations (unmeasurable by depth sensors, boundary views of Kinects). Performance is very low without combing multiple Kinects.

Table 12
Performance of on-line fall detection (%) using RGB and skeleton from Kinect's views.

Kinect view	Acc	Pre	Sens	Spec
Kinect 2	88.89	90.00	87.50	90.00
Kinect 3	84.21	90.91	75.00	83.33
Both Kinects	**91.49**	**92.59**	**90.00**	**92.59**

5.5. *Empirical validation of on-line system with multiple Kinects*

We invited ten volunteers aging from 25 to 45 to evaluate the on-line system. Each person plays free and continuous actions without resetting the system. Different persons play actions in different times (morning, afternoon) of different days. In total, there are twenty seven falls, and twenty non-fall activities (bending, sitting on the chair, leaping, sitting on the bed, object grasping). The activities have been performed continuously without stop. The subject worn different clothes and performed the activities in different duration and at different positions in the room. This scenario is relatively similar to daily life.

An log activities of an empirical validation is illustrated in Fig. 16. In this example, the subject implemented a series of both fall and fall-like events. Corresponding results of the proposed system are given. We then evaluate the proposed system with all of the subjects.

Table 12 shows performance of the whole system (combined RGB and Skeleton, with two Kinect views). More than 90% falls

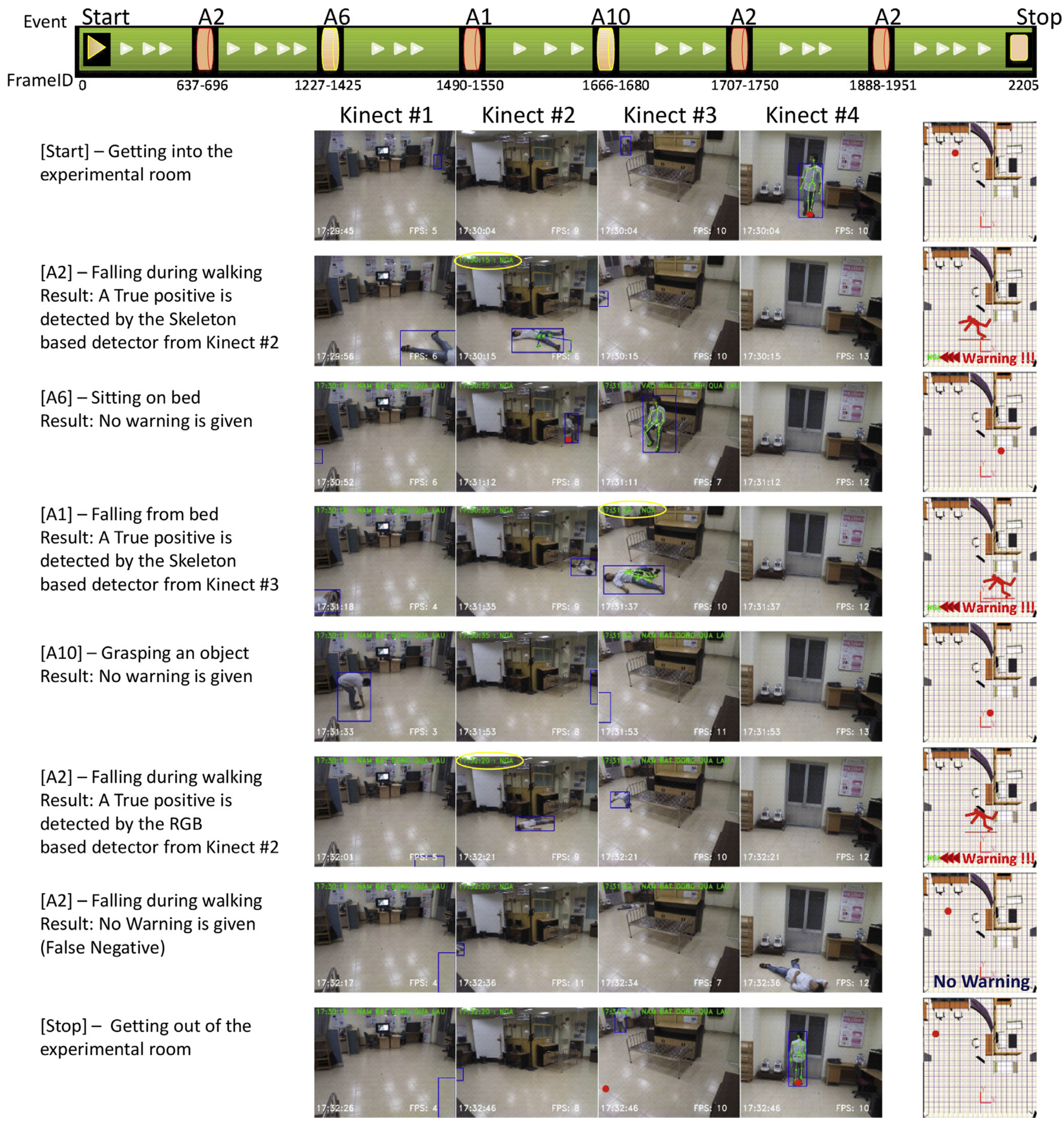

Fig. 16. Log activities of an empirical validation on the proposed system. The top bar indicates events and frame IDs during a trial. For each event, its descriptions and the detection results are given in lower rows. The collected frames from four Kinects at the middle frame of each event are displayed. The processing time (fps) is given on each collected frames. The last column shows a corresponding snapshot of the coordinate PC. Red points indicate current position of the subject. (For interpretation of the references to colour in this figure legend, the reader is referred to the web version of this article.)

have been detected. The system performance reduces lightly when running on-line. The first reason is when running on-line, when skeleton is unavailable, the system must call the fall end detection module from RGB data. This module gives many potential fall candidates because it detected only motionless moments. Then all motionless activity such as standing still, sitting still were detected and input to GMM-GiKDES-SVM for fall and non-fall classification. This is not the case of off-line test with segmented videos. The second reason, that affects more on the result, is we computed GMM based on a pre-defined time duration. But the number of consecutive frames during this interval of time is different from each other (depending on the processing rate of the PC) and different from training samples. This leads to missed or false detection. The combination of results from two Kinect views improves significantly the performance of the system than using single Kinect. This performance is promising when we refer to some state of the art works using multiple camera (Sens = 85.10% [45] using four cameras, Sens = 80.60% [46] using three cameras).

5.6. Discussions

Comparing to state of the art methods, the proposed method for fall detection made some differences and advantages. First, it does not require any pre-processing steps such as background subtraction or human detection which are usually very time consuming and sensitive to lighting condition, occlusion, shadow and cluttered background. For example all of recent works presented in [17,47,48] relied on the segmented human regions. As reported in [17], the foreground human detection was affected by background clutter and object occlusion. In addition, the pre-processing time is huge (about 0.35s per frame with Intel Core i7-2600 3.40 GHz processor, 16GB of RAM). The work presented in [49] performed human detection by applying background subtraction on depth map from Kinect sensor. As mentioned previously, depth map is of low resolution and also affected by noise and limited by its measurable range. Second, while many relevant works focused on extracting features from single image stream such as depth [49], skeleton [7], or RGB. Our proposed method combined efficiently two modalities (skeleton and RGB). On the one hand, it speeds up the proposed system at reliable ranges of Kinect. On the other hand, it avoids missing detection at an unmeasurable range of the depth sensor. In case of using only skeleton, our proposed method also outperforms significantly the method presented in [7]. Our method could avoid lot of false positives thanks to the efficient criteria of motion speed and duration. In case we have used RGB information, the use of improved kernel description with SVM classifier outperformed some existing methods. Our previous work presented in [36] showed that our method GMM-iGKDES-SVM on MSRAction3D dataset obtained 91.57% of accuracy (93.95% by Batabyal et al. [24] and 91.25% by Batabyal et al. [25]). This means that our method is comparable in action recognition problem with these methods. In the case of fall / non-fall classification, the comparisons with other methods [16,17] on a published dataset (Dataset-A) (Table 8) show that our method achieved better performance. As our method uses both skeleton and RGB, it can run in day and night condition. Third, temporal activity spotting from a continuous video stream based on motion map is more stable than that in [17] or advantageous than some other sliding based techniques. In [17], the activity spotting based only on the ratio of human box ratio. In case of occlusion, shadow or viewpoint change, this value could be changed leading to the false spotting. Finally, with the design of client-server architecture, this method could be scalable for any size of environment. Although the method is designed for each camera view independently, it could deal with an occlusion of one camera thank to the detection by another camera. Moreover, at some cross-view positions, the skeleton is not reliable, the possibility that a fall to be detected by one or more camera is increased when using multiple cameras. Existing methods using multiple cameras aims to avoid this situation such as [47] by building 3D silhouette distribution was more complicated and required overlapped camera views.

However, the current system has some limitations. First, it concludes a fall or non-fall based on skeleton if this one is available. However, it did not verify the reliability of skeletons during fall, this leads to some mis-detections. To overcome this limitation, we will conclude only fall based on skeleton, the non-fall conclusion will be checked by GMM-GiKDES-SVM. This is more time-consuming but it avoids to miss-detect fall which is of most important. The second limitation is the GMM computed for an online fall activity is different from off-line segmented video due to the difference in frame rate of acquisition at runtime and at offline training. It could be resolved by implementing multi-threads: one buffering all coming frames and one taking frames from buffer for processing. In the future, we will improve the system with these propositions, combine hand designed features with features extracted from deep learning, extend the method for abnormal behavior detection and analysis of one or multiple people and evaluate with other datasets. The third limitation is that although Kinect sensor is low-cost, however, deployment of the current system in reality is quite expensive because each Kinect sensor has to be connected to one PC. In addition, the spatial configuration of Kinects was not deeply optimized. Moreover, actually, we have not optimized to obtain highest running speed. Aspect real-time should be more studied in future work. The fact that many real practical demonstrations have shown immediately response in the proposed system (for example, a supplemental video is attached). Then, we would like to convince that 10 fps processing time is enough to achieve a real-time performance in practical application. The fourth limitation is that the current system works with the assumption of only one person present in the environment. This assumption is acceptable in reality where much people live alone in home. In case there are many people in the environment, each person should be localized first then the region of interest surrounding each detected human will be processed in the step of activity recognition. Finally, in term of privacy, our method extract features from both skeleton and RGB data. This could be a barrier and not acquiescent by direct users (patient, elderly people). However, we will convince the users by the fact that all acquired data are processed and only avatar and text are displayed or sent to monitors.

6. Conclusions

We presented a new method using multi-modal features from Kinect sensor for fall detection. The proposed method combined RGB and skeleton information in a flexible way. This combination speeds up significantly the system while ensuring the monitoring at positions out of measurable range of depth sensors. The experiments showed that kernel descriptor extracted from gray-scale motion map and rules based detector outperforms state of the art methods for fall and non fall classification. We have deployed this method in a large space using multiple Kinect sensors for continuous fall detection. Compared to previous works, the proposed system can be scalable and reliable and has potential to be applied in reality.

Conflict of interest

We would like to confirm no conflict of interest, financial or other, exists. This manuscript is entirely original, has not been copyrighted, published, submitted, or accepted for publication elsewhere. We have included acknowledgements and funding sources after the conclusion.

Acknowledgment

This research is funded by Vietnam National Foundation for Science and Technology Development (NAFOSTED) under grant number 102.04-2013.32.

Supplementary material

Supplementary material associated with this article can be found, in the online version, at 10.1016/j.cmpb.2017.05.007.

References

[1] R. Igual, C. Medrano, I. Plaza, Challenges, issues and trends in fall detection systems, Biomed. Eng. Online 12 (2013) 66, doi:10.1186/1475-925X-12-66.
[2] M. Mubashir, L. Shao, L. Seed, A survey on fall detection: principles and approaches, Neurocomputing 100 (2013) 144–152, doi:10.1016/j.neucom.2011.09.037.
[3] A. Bourke, J. Obrien, G. Lyons, Evaluation of a threshold-based tri-axial accelerometer fall detection algorithm, Gait Posture 26 (2) (2007) 194–199.

[4] M. Kangas, A. Konttila, I. Winblad, T. Jämsä, Determination of simple thresholds for accelerometry-based parameters for fall detection, in: Annual International Conference of the IEEE Engineering in Medicine and Biology - Proceedings, 2007, pp. 1367–1370, doi:10.1109/IEMBS.2007.4352552.
[5] C.C. Yang, Y.L. Hsu, A review of accelerometry-based wearable motion detectors for physical activity monitoring, 2010,. 10.3390/s100807772.
[6] F. Bagala, C. Becker, A. Cappello, L. Chiari, K. Aminian, J.M. Hausdorff, W. Zijlstra, J. Klenk, Evaluation of accelerometer-based fall detection algorithms on real-world falls, PLoS ONE 7 (2012), doi:10.1371/journal.pone.0037062.
[7] C. Kawatsu, J. Li, C. Chung, Development of a fall detection system with microsoft kinect, in: Robot Intelligence Technology and Applications, Springer, 2012, pp. 623–630, doi:10.1007/978-3-642-37374-9_59.
[8] M. Kepski, B. Kwolek, Unobtrusive fall detection at home using kinect sensor, in: International Conference on Computer Analysis of Images and Patterns, Springer, 2013, pp. 457–464, doi:10.1007/978-3-642-40261-6_55.
[9] G. Mastorakis, D. Makris, Fall detection system using Kinect's infrared sensor, J. Real-Time Image Process. 9 (2012) 635–646, doi:10.1007/s11554-012-0246-9.
[10] S. Gasparrini, E. Cippitelli, S. Spinsante, E. Gambi, A depth-based fall detection system using a kinect® sensor, Sensors 14 (2014) 2756–2775, doi:10.3390/s140202756.
[11] H. Alzoubi, N. Ramzan, H. Shahriar, R. Alzubi, R. Gibson, A. Amira, Optimization and evaluation of the human fall detection system, 2016, 10.1117/12.2242162.
[12] Z. Zhang, C. Conly, V. Athitsos, A survey on vision-based fall detection, in: Proceedings of the 8th ACM International Conference on PErvasive Technologies Related to Assistive Environments PETRA'15, ACM, New York, NY, USA, 2015, pp. 46:1–46:7, doi:10.1145/2769493.2769540.
[13] B. Mirmahboub, S. Samavi, N. Karimi, S. Shirani, Automatic monocular system for human fall detection based on variations in silhouette area, IEEE Trans. Biomed. Eng. 60 (2013) 427–436, doi:10.1109/TBME.2012.2228262.
[14] W. Feng, R. Liu, M. Zhu, Fall detection for elderly person care in a vision-based home surveillance environment using a monocular camera, Signal Image Video Process. 8 (2014) 1129–1138, doi:10.1007/s11760-014-0645-4.
[15] I. Charfi, J. Miteran, J. Dubois, M. Atri, R. Tourki, Optimized spatio-temporal descriptors for real-time fall detection: comparison of support vector machine and adaboost-based classification, J. Electron. Imaging 22 (4) (2013) 041106.
[16] Y. Yun, I.Y.-H. Gu, Human fall detection via shape analysis on riemannian manifolds with applications to elderly care, in: IEEE International Conference on Image Processing (ICIP), 2015, pp. 3280–3284.
[17] Y. Yun, I.Y.-H. Gu, Human fall detection in videos via boosting and fusing statistical features of appearance, shape and motion dynamics on riemannian manifolds with applications to assisted living, Comput. Vision Image Understanding 148 (2016) 111–122.
[18] C. Rougier, J. Meunier, A. St-Arnaud, J. Rousseau, Fall detection from human shape and motion history using video surveillance, in: 21st International Conference on Advanced Information Networking and Applications Workshops (AINAW'07), 2, 2007, pp. 875–880, doi:10.1109/AINAW.2007.181.
[19] E. Auvinet, F. Multon, A. St-Arnaud, J. Rousseau, J. Meunier, Fall detection using body volume reconstruction and vertical repartition analysis., in: International conference on Image and signal processing, 2010, pp. 376–383, doi:10.1007/978-3-642-13681-8.
[20] D. Anderson, R.H. Luke, J.M. Keller, M. Skubic, M. Rantz, M. Aud, Linguistic summarization of video for fall detection using voxel person and fuzzy logic, Comput. Vision Image Understanding 113 (2009) 80–89, doi:10.1016/j.cviu.2008.07.006.
[21] N. Thome, S. Miguet, S. Ambellouis, A real-time, multiview fall detection system: a LHMM-based approach, IEEE Trans. Circuits Syst. Video Technol. 18 (2008) 1522–1532, doi:10.1109/TCSVT.2008.2005606.
[22] S. Zambanini, J. Machajdik, M. Kampel, Early versus Late Fusion in a Multiple Camera Network for Fall Detection, in: Computer Vision in a Global Society - 34th Annual Workshop of the Austrian Association for Pattern Recognition (AAPR) and the WG Visual Computing of the Austrian Computer Society, 2010, pp. 15–22.
[23] X. Ma, H. Wang, B. Xue, M. Zhou, B. Ji, Y. Li, Depth-based human fall detection via shape features and improved extreme learning machine, IEEE J. Biomed. Health Inf. 18 (6) (2014) 1915–1922, doi:10.1109/JBHI.2014.2304357.
[24] T. Batabyal, A. Vaccari, S.T. Acton, Ugrasp: a unified framework for activity recognition and person identification using graph signal processing, in: 2015 IEEE International Conference on Image Processing (ICIP), IEEE, 2015a, pp. 3270–3274.
[25] T. Batabyal, T. Chattopadhyay, D.P. Mukherjee, Action recognition using joint coordinates of 3d skeleton data, in: Image Processing (ICIP), 2015 IEEE International Conference on, IEEE, 2015b, pp. 4107–4111.
[26] Y. Du, W. Wang, L. Wang, Hierarchical recurrent neural network for skeleton based action recognition, in: Proceedings of the IEEE Conference on Computer Vision and Pattern Recognition, 2015, pp. 1110–1118.
[27] C. Wang, Y. Wang, A.L. Yuille, Mining 3d key-pose-motifs for action recognition, in: Proceedings of the IEEE Conference on Computer Vision and Pattern Recognition (CVPR), 2016, pp. 2639–2647.
[28] L. Lo Presti, M. La Cascia, 3d skeleton-based human action classification, Pattern Recognit. 53 (C) (2016) 130–147.
[29] M.M. Flores-Barranco, M.-A. Ibarra-Mazano, I. Cheng, Accidental fall detection based on skeleton joint correlation and activity boundary, in: International Symposium on Visual Computing, Springer, 2015, pp. 489–498, doi:10.1007/978-3-319-27863-6_45.
[30] T.-H. Tran, T.-L. Le, J. Morel, An analysis on human fall detection using skeleton from microsoft kinect, in: IEEE Fifth International Conference on Communications and Electronics (ICCE), 2014, pp. 484–489, doi:10.1109/CCE.2014.6916752.
[31] G. Mastorakis, D. Makris, Fall detection system using kinect's infrared sensor, J. Real-Time Image Process. 9 (4) (2012) 635–646, doi:10.1007/s11554-012-0246-9.
[32] M. Kepski, B. Kwolek, Fall detection using ceiling-mounted 3d depth camera, in: International Conference on Computer Vision Theory and Applications (VISAPP), 2, IEEE, 2014, pp. 640–647.
[33] B. Kwolek, M. Kepski, Human fall detection on embedded platform using depth maps and wireless accelerometer, Comput. Methods Programs Biomed. 117 (2014) 489–501, doi:10.1016/j.cmpb.2014.09.005.
[34] B. Kwolek, M. Kepski, Improving fall detection by the use of depth sensor and accelerometer, Neurocomputing 168 (2015) 637–645, doi:10.1016/j.neucom.2015.05.061.
[35] R. Cucchiara, A. Prati, R. Vezzani, A multi-camera vision system for fall detection and alarm generation, Expert Syst. 24 (5) (2007) 334–345, doi:10.1111/j.1468-0394.2007.00438.x.
[36] T.-H. Tran, V.-T. Nguyen, How good is Kernel descriptor on depth motion map for action recognition, in: The 10th International Conference on Computer Vision Systems, 2015, pp. 137–146, doi:10.1007/978-3-319-20904-3_13.
[37] X. Yang, C. Zhang, Y. Tian, Recognizing actions using depth motion maps-based histograms of oriented gradients, in: The 20th ACM International Conference on Multimedia, 2012, pp. 1057–1060, doi:10.1145/2393347.2396382.
[38] C. ChenR. Jafari, N. Kehtarnavaz, Action recognition from depth sequences using depth motion maps-based local binary patterns, in: IEEE Winter Conference on Applications of Computer Vision, 2015, pp. 1092–1099, doi:10.1109/WACV.2015.150.
[39] L. Bo, X. Ren, D. Fox, Kernel descriptors for visual recognition, in: Advances in Neural Information Processing Systems, 2010, pp. 244–252.
[40] V.-T. Nguyen, T.-L. Le, T.-T.-H. Tran, M. Remy, C. Vincent, A new hand representation based on Kernels for hand posture recognition, in: The Eleventh IEEE International Conference on Automatic Face and Gesture Recognition, 2015, pp. 1–6, doi:10.1109/FG.2015.7163110.
[41] H.-G. Doan, H. Vu, T.-H. Tran, E. Casteli, Improvements of RGB-D Hand posture recognition using an user-guide scheme, in: IEEE 7th International Conference on Cybernetics and Intelligent Systems (CIS) and IEEE Conference on Robotics, Automation and Mechatronics (RAM), 2015, pp. 24–29, doi:10.1109/ICCIS.2015.7274542.
[42] T.T.T. Pham, T.L. Le, T.K. Dao, D.H. Le, A robust model for person re-identification in multimodal person localization, in: The 9th International Conference on Mobile Ubiquitous Computing, Systems, Services and Technologies, 2015, pp. 38–43.
[43] http://mica.edu.vn/perso/Tran-Thi-Thanh-Hai/MFD.html.
[44] http://www.robofest.net/FDR/.
[45] J. Machajdik, S. Zambanini, M. Kampel, Fusion of data from multiple cameras for fall detection, in: Workshop on Behaviour Monitoring and Interpretation, 2010, pp. 1–7.
[46] E. Auvinet, F. Multon, A. Saint-Arnaud, J. Rousseau, J. Meunier, Fall detection with multiple cameras: an occlusion-Resistant method based on 3-D silhouette vertical distribution, IEEE Trans. Inf. Technol.Biomed. 15 (2) (2011a) 290–300, doi:10.1109/TITB.2010.2087385.
[47] E. Auvinet, F. Multon, A. Saint-Arnaud, J. Rousseau, J. Meunier, Fall detection with multiple cameras: an occlusion-resistant method based on 3-d silhouette vertical distribution, IEEE Trans. Inf. Technol. Biomed. 15 (2) (2011b) 290–300.
[48] J.-L. Chua, Y.C. Chang, W.K. Lim, A simple vision-based fall detection technique for indoor video surveillance, Signal Image Video Process. 9 (3) (2015) 623–633.
[49] E. Stone, M. Skubic, Fall detection in homes of older adults using the microsoft kinect, IEEE J. Biomed. Health Inf. 19 (2014) 290–301, doi:10.1109/JBHI.2014.2312180.

Computer Methods and Programs in Biomedicine

Country	Netherlands
Subject Area and Category	Computer Science Computer Science Applications Software Medicine Health Informatics
Publisher	Elsevier BV
Publication type	Journals
ISSN	01692607
Coverage	1985-ongoing
Scope	To encourage the development of formal computing methods, and their application in biomedical research and medical practice, by illustration of fundamental principles in biomedical informatics research; to stimulate basic research into application software design; to report the state of research of biomedical information processing projects; to report new computer methodologies applied in biomedical areas; the eventual distribution of demonstrable software to avoid duplication of effort; to provide a forum for discussion and improvement of existing software; to optimize contact between national organizations and regional user groups by promoting an international exchange of information on formal methods, standards and software in biomedicine. (source)

71

H Index

Quartiles +

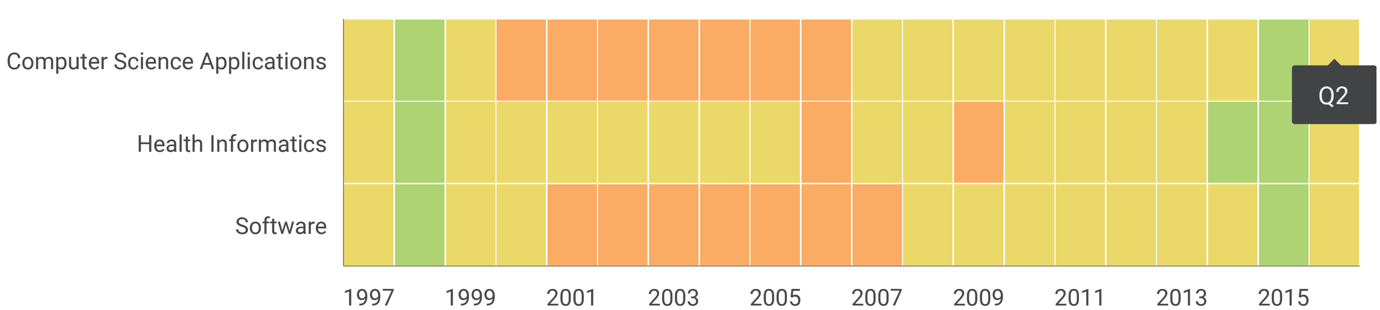

SJR +

Citations per document +

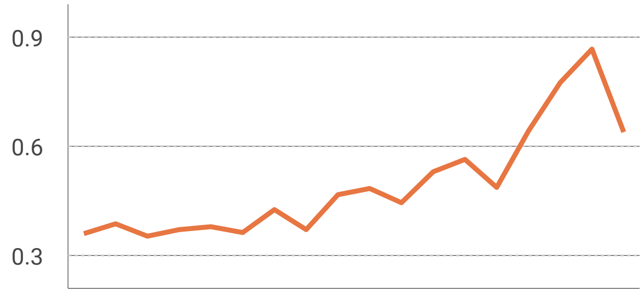

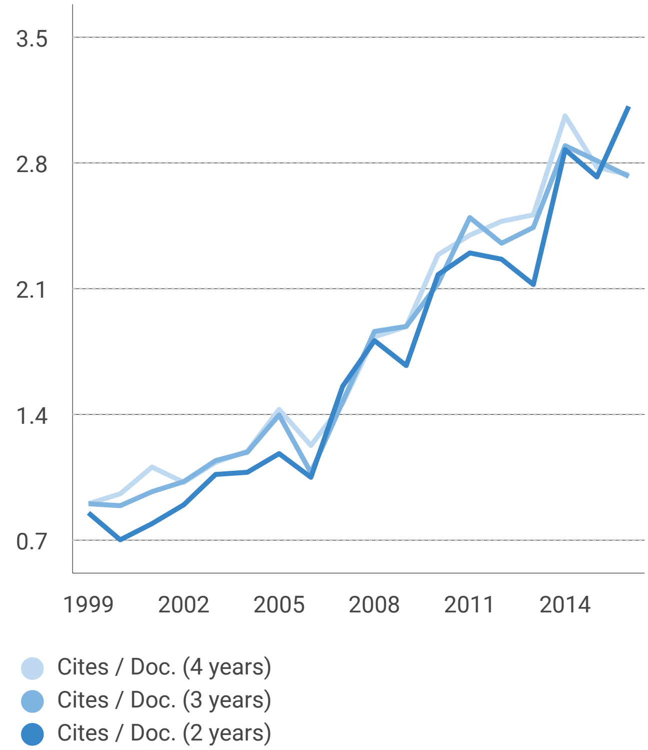

Total Cites Self-Cites

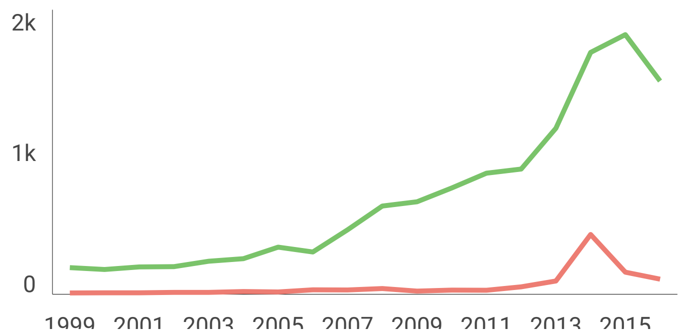

External Cites per Doc Cites per Doc

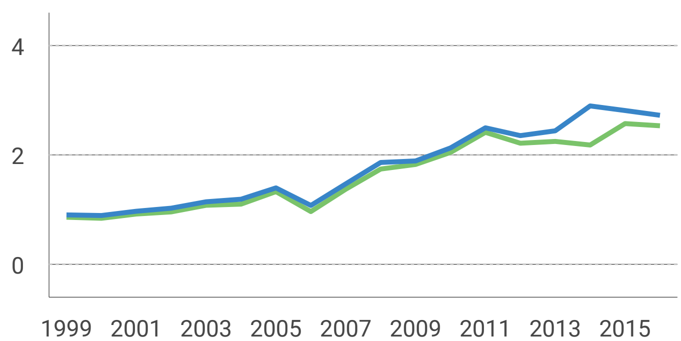

% International Collaboration

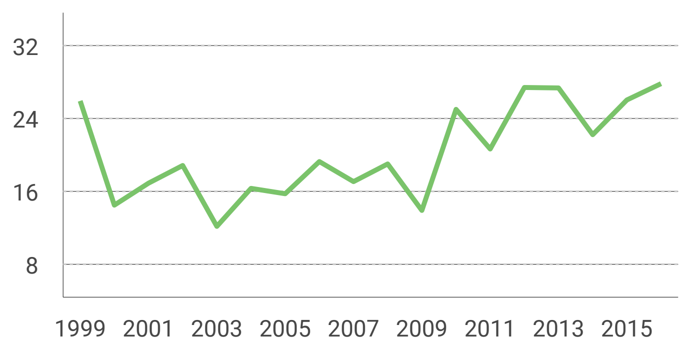

Citable documents Non-citable documents

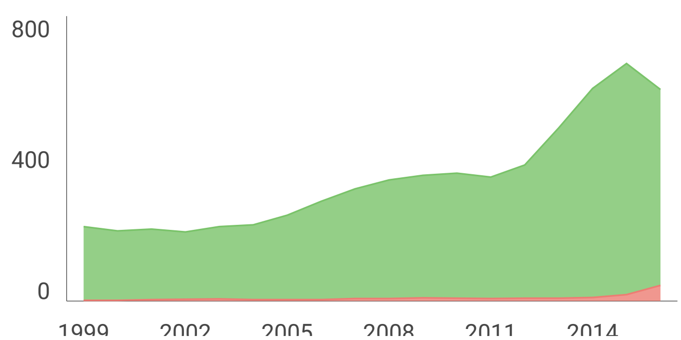

Cited documents Uncited documents

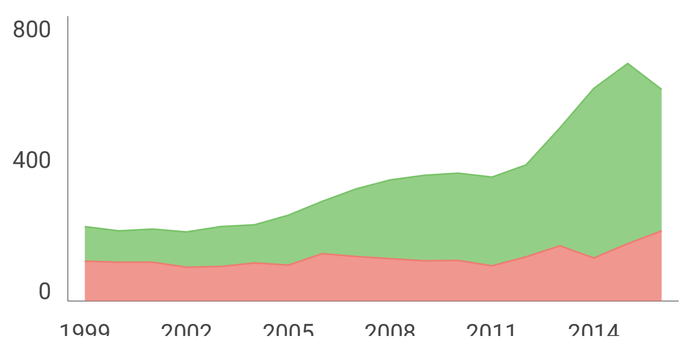

Show this widget in your own website

Just copy the code below and paste within your html code:

<a href="http://www.scimag

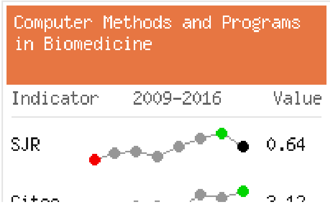
Computer Methods and Programs in Biomedicine
Indicator
2009-2016
Value
SJR
0.64

- Support
- Contact Us
- Corporate website

Site

Client

proxystylesheet

Output

Search Site Search

allAreas

JOURNAL SEARCH

SCIENCE CITATION INDEX - COMPUTER SCIENCE, INTERDISCIPLINARY APPLICATIONS - JOURNAL LIST

Total journals: 31

Journals 1-10 (of 31)

FORMAT FOR PRINT

- **COMPUTATIONAL BIOLOGY AND CHEMISTRY**
  Bimonthly ISSN: 1476-9271
  ELSEVIER SCI LTD, THE BOULEVARD, LANGFORD LANE, KIDLINGTON, OXFORD, ENGLAND, OXON, OX5 1GB
  Coverage
  - Science Citation Index
  - Science Citation Index Expanded
  - Current Contents - Life Sciences
  - BIOSIS Previews
- **COMPUTATIONAL LINGUISTICS**
  Quarterly ISSN: 0891-2017
  MIT PRESS, ONE ROGERS ST, CAMBRIDGE, USA, MA, 02142-1209
  Coverage
  - Science Citation Index
  - Science Citation Index Expanded
  - Social Sciences Citation Index
  - Arts & Humanities Citation Index
  - Current Contents - Engineering, Computing & Technology
  - Current Contents - Arts & Humanities
- **COMPUTER METHODS AND PROGRAMS IN BIOMEDICINE**

Monthly ISSN: 0169-2607
ELSEVIER IRELAND LTD, ELSEVIER HOUSE, BROOKVALE PLAZA, EAST PARK SHANNON, CO, CLARE, IRELAND, 00000
Coverage
  - Science Citation Index
  - Science Citation Index Expanded
  - Current Contents - Life Sciences
  - BIOSIS Previews

- **COMPUTER MUSIC JOURNAL**
  Quarterly ISSN: 0148-9267
  MIT PRESS, ONE ROGERS ST, CAMBRIDGE, USA, MA, 02142-1209
  Coverage
  - Science Citation Index
  - Science Citation Index Expanded
  - Arts & Humanities Citation Index
  - Current Contents - Arts & Humanities

- **COMPUTER PHYSICS COMMUNICATIONS**
  Monthly ISSN: 0010-4655
  ELSEVIER SCIENCE BV, PO BOX 211, AMSTERDAM, NETHERLANDS, 1000 AE
  Coverage
  - Science Citation Index
  - Science Citation Index Expanded
  - Current Contents - Physical, Chemical & Earth Sciences

- **COMPUTERS & CHEMICAL ENGINEERING**
  Monthly ISSN: 0098-1354
  PERGAMON-ELSEVIER SCIENCE LTD, THE BOULEVARD, LANGFORD LANE, KIDLINGTON, OXFORD, ENGLAND, OX5 1GB
  Coverage
  - Science Citation Index
  - Science Citation Index Expanded
  - Current Contents - Engineering, Computing & Technology

- **COMPUTERS & FLUIDS**
  Monthly ISSN: 0045-7930
  PERGAMON-ELSEVIER SCIENCE LTD, THE BOULEVARD, LANGFORD LANE, KIDLINGTON, OXFORD, ENGLAND, OX5 1GB
  Coverage
  - Science Citation Index
  - Science Citation Index Expanded
  - Current Contents - Engineering, Computing & Technology

- **COMPUTERS & GEOSCIENCES**
  Monthly ISSN: 0098-3004
  PERGAMON-ELSEVIER SCIENCE LTD, THE BOULEVARD, LANGFORD LANE, KIDLINGTON, OXFORD, ENGLAND, OX5 1GB
  Coverage
  - Science Citation Index

- Science Citation Index Expanded
- Current Contents - Physical, Chemical & Earth Sciences

- **COMPUTERS & STRUCTURES**
  Monthly ISSN: 0045-7949
  PERGAMON-ELSEVIER SCIENCE LTD, THE BOULEVARD, LANGFORD LANE, KIDLINGTON, OXFORD, ENGLAND, OX5 1GB
  Coverage
  - Science Citation Index
  - Science Citation Index Expanded
  - Current Contents - Engineering, Computing & Technology

- **COMPUTERS IN BIOLOGY AND MEDICINE**
  Monthly ISSN: 0010-4825
  PERGAMON-ELSEVIER SCIENCE LTD, THE BOULEVARD, LANGFORD LANE, KIDLINGTON, OXFORD, ENGLAND, OX5 1GB
  Coverage
  - Science Citation Index
  - Science Citation Index Expanded
  - Current Contents - Life Sciences
  - BIOSIS Previews

Journals 1-10 (of 31)

FORMAT FOR PRINT